On the eigenvalue distribution of the Sachdev-Ye-Kitaev Model

Martin Roelfs
Supervised by prof. dr. K. Papadodimas
Co-advisor: prof. dr. E.A. Bergshoeff

November 2, 2016

Contents

Chapter 1

Introduction

The study of black holes is of great importance in furthering our understanding of quantum gravity. This is because in order to describe black holes properly, both Quantum Mechanics (QM) and General Relativity (GR) are needed. But the union of these two theories keeps throwing up paradoxes, and in solving them, our understanding of nature is pushed forward.

In this section, some of these paradoxes will be outlined, as well as some of the theoretical tools used to study them. All this will make it clear that toy models are needed to help futher our understanding of these difficult topics. And it appears that such a toy model might have been found: the Sachdev-Ye-Kitaev (SYK) model.

Perhaps the most important paradox is the Hawking Information paradox. It stems from Hawking's calculation that black holes evaporate, leaving behind nothing but thermal radiation, now commonly called *Hawking radiation*. The evaporation suggests that all the information that ever fell into the black hole is now gone, since classically there can be no information in thermal radiation. This contradicts the unitarity of Quantum Mechanics, which suggests that information should be conserved.

However, Hawking's calculations were semi-classical. Therefore, unitarity could be preserved, if there is a small amount of quantum entanglement in the Hawking radiation. This way it would still appear thermal, yet it would contain all the information of the original black hole. Such entanglement of the Hawking radiation would therefore solve the paradox.

But in a now classic paper by Almheiri, Marolf, Polchinski, and Sully, it was suggested that this solution of the Hawking paradox leads to a contradiction with a cornerstone prediction of GR: black holes should have smooth horizons. Instead they claim that the entangled Hawking radiation leads to a *firewall*[1]: a seething hot mass of particles on the horizon that would evaporate anything trying to cross the horizon. This has been dubbed the firewall paradox.

The firewall appears because it can be shown that in order for the black hole horizon to be smooth, as predicted by GR, the Quantum Field Theory (QFT) inside and outside the black hole have to be entangled. If this entanglement is broken, the horizon cannot be smooth, and instead a firewall appears[2]. But as argued before, the Hawking radiation has to be entangled in order for information to be conserved.

Because of monogamy of entanglement only one of these two statements can

be true. Therefore, the information paradox rises again: either black holes have smooth horizons but information is lost through evaporation, *or* information is conserved but black holes have a firewall and horizons are everything but smooth.

In investigating these paradoxes, new theoretical tools have been developed. Arguably the greatest among them is *holography*. Because of pioneering work by Hawking and Bekenstein, it became clear that black holes have temperature and therefore entropy. This entropy scales with the surface area of the black hole, rather than its volume. And since entropy is a measure of our ignorance – of the amount of information we *don't* know – this suggests that all the information that ever fell into the black hole is encoded on the horizon, not in the volume. This radical insight led to the idea of holography; perhaps all the information in a certain number of dimensions could be encoded in one dimension less.

The only concrete example of a theory where this seems to hold, is the AdS/CFT duality[3]. It was proposed by Maldacena through string theory, that in the large N limit, a d dimensional Conformal Field Theory (CFT), is equivalant to gravity in $d+1$ dimensional Anti-de Sitter (AdS) space. Quantum gravitational computations done in the AdS bulk are then dual to QFT calculations done in the CFT. The true power of AdS/CFT is that it inverts the coupling strength; weakly coupled gravity is dual to a strongly coupled CFT and vise versa. This allows calculations to be performed on strongly coupled theories, something for which no other computational tools are available.

However, such calculations are subject to a lot of constraints, and the AdS-CFT mapping is still not fully understood. Therefore, toy models are in demand. Similarly, the firewall paradox makes studying the exact nature of themalization of black holes important. Just like in classical systems, it turns out that thermalization of quantum systems occurs through chaotic processes (Section 1.1). But unlike in classical chaos, it can be shown that there is an upper bound on quantum chaos[4]. Black holes saturate this bound and are believed to be optimal scramblers of information[5, 6, 7, 8]. Therefore, toy models of quantum chaos are also in high demand.

Recently the Sachdev-Ye-Kitaev (SYK) Hamiltonian has been proposed by Kitaev[9] as a toy model for both holography and quantum chaos. The SYK model is a $0+1$ dimensional model of N fermions with random quartic all-to-all interactions. Rather uniquely, the model becomes solvable at strong coupling, and has an emergent conformal CFT_1 symmetry. Therefore, it could have a holographicly dual AdS_2. Additionally, it is chaotic, and satisfies the upper bound on quantum chaos just like black holes do[9].

Any one of the aforementioned qualities would have made studying this model worthwhile. But the combination of all three in a single model has sparked an incredible research interest into this model.

The Hamiltonian as proposed by Kitaev is given in (1.1).

$$\mathcal{H} = \sum_{1\leq i<j<k<l\leq N} J_{ijkl}\chi_i\chi_j\chi_k\chi_l \tag{1.1}$$

$$J_{ijkl} \sim \mathcal{N}\left(\mu = 0, \sigma^2 = \frac{3!J^2}{N^3}\right) \tag{1.2}$$

In this Hamiltonian the χ_i are fermionic fields satisfying $\{\chi_i, \chi_j\} = \delta_{ij}$, and the J_{ijkl} are drawn from a Gaussian distribution.

It has been shown that this Hamiltonian can be solved exactly at strong coupling or equivalently in the low energy limit[9], for large N. This means we would like to investigate the low energy limit of this model, and in particular the ground state and the first couple of excited states. A very natural question to ask is therefore: can we directly calculate the eigenvalue distribution of the Hamiltonian?

This thesis explores this question by looking at the eigenvalue distributions of a one and a two fermion analog of the SYK Hamiltonian. Finally some connections with the four fermion model will be made.

The (uninteracting) one fermion model has been solved exactly, and showed a method for solving the more interesting two fermion model. However, using the tools developed for the one fermion model, we were unable to solve the eigenvalue distribution of the two fermion model. Nevertheless it yielded some very interesting results; most importantly that all higher interaction models have in them a part that behaves like the one fermion model (whose behavior is known exactly). Although in general this part becomes unimportant in the large N limit, it does seem to suggest that if in the large N limit we look at the $N-1$ fermion interaction, the system might still have the desired chaotic behavior and the eigenvalue distribution would that of the solved one fermion model. This would therefore be very interesting follow-up research.

1.1 Quantum Chaos

Systems that are prepared out of thermodynamic equilibrium, will reach thermodynamic equilibrium via chaotic processes. This is called *thermalization*. A system is said to be in thermodynamic equilibrium when all microstates of the system are equiprobable.

In classical systems, chaos is defined by a strong dependence on initial conditions; only slightly different initial conditions can produce wildly different results.

In order to decribe how chaos causes thermalization, let us consider a system that was prepared to occupy a very specific spherical region of phase space. Imagine for example, an ideal gas in which all the particles have very similar momenta and start of at roughly the same position.

Due to the strong dependence on the initial conditions, two particles that are initialized almost exactly the same, will evolve very differently over time. As time passes, their phase space coordinates will diverge. As a result, the initial spherical blob these particles occupied in phase space, will spread out and become more diffuse in phase space, while keeping the total volume it occupies the same due to Liouville's theorem. At large times, the initial blob will therefore evolve into thin filaments occupying all of the hypersurface allowed by conservation laws.

To quantify this, one can look at the Lyapunov exponent of the system. This is a measure of the rate of divergence for trajectories that were initially arbitrarily close. For example, for the evolution of position with time

$$\frac{\partial q(t)}{\partial q(0)} \approx e^{\lambda_L t} \tag{1.3}$$

where $q(t)$ is the seperation between two points at time t, and λ_L is the Lyapunov exponent.

Looking at (1.3), it can be observed that $\frac{\partial q(t)}{\partial q(0)} = \{q(t), p(0)\}$, the Poisson bracket. This seems to suggest that, using the canonical quantization procedure, it is $\frac{1}{i\hbar}[\hat{q}(t), \hat{p}(0)]$ that should grow exponentially in quantum chaos.

But since Quantum Mechanics is linear and therefore unitary, it might seem like there is no such thing as Quantum Chaos in the first place. After all, the overlap between two states remains the same under time evolution, since $|\phi(t)\rangle = \exp[-i\mathcal{H}t/\hbar]\,|\phi(0)\rangle$. However, orthogonal states can appear to be physically similar, but this similarity does not have to be preserved under unitary evolution. Therefore, the resemblance of such states could diverge exponentially.

Because $\langle[\hat{x}(t), \hat{p}(0)]\rangle$ will in general be zero due to phase cancellation, a better definition is $\langle[\hat{x}(t), \hat{p}(0)]^\dagger\,[\hat{x}(t), \hat{p}(0)]\rangle$. Here $\langle\hat{A}\rangle$ denotes the thermal average of the operator $\hat{A}$, given by

$$\left\langle \hat{A} \right\rangle = \mathrm{tr}\left(\rho\hat{A}\right) = \frac{\mathrm{tr}\left(e^{-\beta\mathcal{H}}\hat{A}\right)}{\mathrm{tr}\left(e^{-\beta\mathcal{H}}\right)} \tag{1.4}$$

Therefore, if a quantum system is chaotic, we would expect the commutator-squared to grow as

$$\left\langle \left|\,[W(t), V(0)]\,\right|^2 \right\rangle \sim e^{2\lambda_L t} \tag{1.5}$$

where we have generalized to any pair of operators W and V.

This growth cannot continue unbounded; at large enough t thermal equilibrium is established, at which point we would expect the commutator (1.5) to stabilize. By analyzing the terms in (1.5), it seems reasonable to expect the commutator to be zero initially, then grow exponentially as (1.5), and finally for it to assume a constant value at thermal equilibrium.

This means that the out-of-time-order terms $\langle W(t)V(0)W(t)V(0)\rangle$, should decrease in size exponentially until they reach zero at large t, since no correlation is expected between states separated by a large time interval in a strongly interacting system (at finite temperature).

Therefore, for t large enough, thermal equilibrium is given by the time ordered part of (1.5):

$$\left\langle \left|\,[W(t), V(0)]\,\right|^2 \right\rangle \to 2\,\langle VV\rangle\,\langle WW\rangle \tag{1.6}$$

In the particular case of the Majorana fermions in the SYK Hamiltonian, two obvious choices for the operators W and V would be χ_i and π_j. However, the conjugate momentum π_j is given by $\pi_j = i\chi_j$. Therefore, the four point function of interest is $\langle\chi_i(t_1)\chi_j(t_2)\chi_i(t_3)\chi_j(t_4)\rangle$. Such four-point functions will be reviewed in 2.5.

Surprisingly, (1.6) suggests that quantum chaos has an upper-bound unlike classical chaos. Indeed, it was conjectured by Maldancena, Shenker and Stanford that there exists such an upper bound, and that quantum chaos can grow no faster than exponentially with a Lyapunov exponent of $\lambda_L \leq 2\pi k_B T/\hbar$[4]. Since black holes are conjectured to be the fastest scramblers in nature, they saturate this bound[6].

1.2 The SYK Hamiltonian

For q fermions the general SYK Hamiltonian is

$$\mathcal{H} = i^{q(q-1)/2} \sum_{\mu_1>\mu_2>\ldots>\mu_q} J_{\mu_1\mu_2\ldots\mu_q}\chi_{\mu_1}\chi_{\mu_2}\cdots\chi_{\mu_q} \tag{1.7}$$

$$J_{\mu_1\mu_2\ldots\mu_q} \sim \mathcal{N}\left(\mu = 0, \sigma^2 = \frac{J^2(q-1)!}{N^{q-1}}\right) \tag{1.8}$$

with $\{\chi_i, \chi_j\} = \delta_{ij}$ and $J_{\mu_1\mu_2\ldots\mu_q}$ a random coupling constant drawn from a Gaussian distribution. A factor of i is included to make the Hamiltonian Hermitian when $2, 3 \equiv q \mod 4$. In this form, also odd q are allowed.

Naively one might expect that since the SYK Hamiltonian is the sum of Gaussian variables, its eigenvalues will be Gaussian distributed. However, this sidesteps the anti-commutative properties of the χ_i, which leads to non-Gaussian behavior.

Numerical simulations show this non-Gaussian behavior at small N (Section 7). However, since $[\chi_i\chi_j\chi_k\chi_l, \chi_{i'}\chi_{j'}\chi_{k'}\chi_{l'}] = 0$ if all indices are different, one would expect such commuting terms to dominate at large N, and therefore Gaussian behavior to reappear.

In this thesis the distribution of the spectrum of SYK-type Hamiltonians is studied for $q = 1$ and $q = 2$. As a toy model the $q = 1$ model is solved exactly in Chapter 4. The $q = 2$ model is studied in Chapter 5.

1.3 Conventions

In this thesis a slightly modified version of (1.7) is used. Observing that the free Majorana fermions are essentially N dimensional Dirac γ matrices[10], and using that $\mu_1 > \mu_2 > \ldots > \mu_q$,

$$\mathcal{H} = i^{q(q-1)/2} \sum_{\mu_1>\mu_2>\ldots>\mu_q} J_{\mu_1\mu_2\ldots\mu_q}\chi_{\mu_1}\chi_{\mu_2}\cdots\chi_{\mu_q} \tag{1.9}$$

$$= \frac{i^{q(q-1)/2}}{q!} \sum_{\mu_1,\mu_2,\ldots,\mu_q} J_{\mu_1\mu_2\ldots\mu_q}\chi^{\mu_1\mu_2\cdots\mu_q} \tag{1.10}$$

$$\chi^{\mu_1\mu_2\cdots\mu_q} = \chi^{[\mu_1}\cdots\chi^{\mu_q]} := \frac{1}{q!}\sum_{\pi\in S_q}\epsilon(\pi)\chi^{\mu_{\pi(1)}}\cdots\chi^{\mu_{\pi(q)}} \tag{1.11}$$

with $J_{\mu_1\mu_2\ldots\mu_q}$ fully antisymmetric, and $\chi^{\mu_1\mu_2\cdots\mu_q}$ the antisymmetric product. This way of writing the Hamiltonian allows the use of all the machinery of antisymmetric products and the Clifford algebra[11, 12]. This is useful in calculating the moments of $q \geq 2$ models.

All methods for calculating with antisymmetric products has been taken from[11], in particular Chapter 3. The choice of Greek indices in this thesis is also based on staying consistent with this book.

1.4 Disorder Averaging

In condensed matter physics, disorder averaging is commonly used to e.g. average out impurities in a lattice. In the SYK model this method is vital to the solvability of the model.

In the SYK model, each $J_{\mu_1\mu_2\ldots\mu_q}$ is drawn from a Gaussian distribution.

$$J_{\mu_1\mu_2\ldots\mu_q} \sim \mathcal{N}\left(\mu = 0, \sigma^2 = \frac{J^2(q-1)!}{N^{q-1}}\right) \tag{1.12}$$

$$\left\langle J^{2k}_{\mu_1\mu_2\ldots\mu_q} \right\rangle = (2k-1)!!\sigma^{2k} \tag{1.13}$$

Since all odd moments are zero, only Feynman diagrams with an even number of vertices will survive the process of disorder averaging.

As a simple example, let consider the simplest non-trivial diagram possible for the $q = 4$ model:

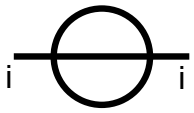

By following the Feynman rules explained in more detail in Chapter 2, it can be seen that the amplitude A is given by:

$$A = J^2_{ijkl}\binom{N-1}{3}G_0(\omega)^3 \tag{1.14}$$

where $G_0(\omega)$ is the free propagator in momentum space and $\binom{N-1}{3}$ counts the total number of unique diagrams of this type. (To see this, remember that i has already been selected. Therefore, there are $N-1$ choices remaining for j. After that, $N-2$ for k, etc.)

Applying the process of disorder averaging by averaging over the J_{ijkl} and using that $N \gg 1$,

$$\langle A \rangle = \left\langle J^2_{ijkl} \right\rangle \binom{N-1}{3} G_0(\omega)^3 \tag{1.15}$$

$$\simeq J^2 G_0(\omega)^3 \tag{1.16}$$

The result is therefore remarkably simple. All amplitudes in this thesis will be after disorder averaging has been applied unless otherwise specified.

Chapter 2

SYK Hamiltonian

The SYK model is given by the Hamiltonian,

$$\mathcal{H} = i^{q(q-1)/2} \sum_{\mu_1 > \mu_2 > \ldots > \mu_q} J_{\mu_1 \mu_2 \ldots \mu_q} \chi_{\mu_1} \chi_{\mu_2} \cdots \chi_{\mu_q} \tag{2.1}$$

$$J_{\mu_1 \mu_2 \ldots \mu_q} \sim \mathcal{N}\left(\mu = 0, \sigma^2 = \frac{J^2 (q-1)!}{N^{q-1}}\right) \tag{2.2}$$

where the χ_i are N Majorana fermion fields, which satisfy $\{\chi_i, \chi_j\} = \delta_{ij}$.

The model is defined in $d = 0 + 1$ spacetime dimension. This means the Lagrangian $\mathcal{L}$ follows trivially as

$$\mathcal{L} = -\frac{1}{2} \chi_j \partial_t \chi_j - \mathcal{H} \tag{2.3}$$

The $q = 4$ model is the model as proposed by Kitaev. Therefore only the correlation functions of $q = 4$ will be studied in this section. However, the results can be generalized to any q[10].

2.1 Free Theory

The generating functional for the free theory is given by

$$Z\left[\vec{\eta}\right] = \int \mathcal{D}\chi_1 \ldots \int \mathcal{D}\chi_N \exp\left[i \int \mathrm{d}t \sum_{j=1}^{N} \left(-\frac{1}{2} \chi_j \partial_t \chi_j + \eta_j \chi_j \right) \right] \tag{2.4}$$

where $\vec{\eta}$ is used to indicate the collection of η_i, the sources of the Majorana fermions. The propagator can be obtained by completing the squares.

$$Z[\eta_j] = \int \mathcal{D}\chi_j e^{i \int \mathrm{d}t \left(-\frac{1}{2} \chi_j \partial_t \chi_j + \eta_j \chi_j \right)} \tag{2.5}$$

$$Z[\eta_j] = \int \mathcal{D}\chi_j e^{-\frac{1}{2} \left(\chi_j + \eta_j \partial_t^{-1} \right) \partial_t \left(\chi_j + \partial_t^{-1} \eta_j \right)} e^{\frac{1}{2} \eta_j \partial_t^{-1} \eta_j} \tag{2.6}$$

$$Z[\eta_j] = C e^{\frac{1}{2} \eta_j \partial_t^{-1} \eta_j} \tag{2.7}$$

The free propagator $G(t_2 - t_1) = \partial_t^{-1}$ is obtained by solving

$$\partial_t G(t_2 - t_1) = \delta(t_2 - t_1) \tag{2.8}$$

A Fourier transform gives

$$\mathcal{F}\left[\partial_t G(t_2 - t_1)\right] = \mathcal{F}\left[\delta(t_2 - t_1)\right] \tag{2.9}$$
$$i\omega \mathcal{F}\left[G(t_2 - t_1)\right] = \mathcal{F}\left[\delta(t_2 - t_1)\right] \tag{2.10}$$
$$i\omega G(\omega) = 1 \tag{2.11}$$

Therefore, in momentum space the free propagator is given by

$$G(\omega) = \frac{1}{i\omega} \tag{2.12}$$

whose Fourier transform in coordinate space is

$$G(t) = -\frac{1}{2}\mathrm{sgn}(t) \tag{2.13}$$

2.2 Two-point Function

By taking a careful look at the allowed Feynman diagrams given by $\mathcal{H}$, the full propagator $G(t_1, t_2)$ can be derived without explicit computation.

Firstly, we notice that after disorder averaging over J_{ijkl}, all Feynman diagrams with an odd number of vertices disappear since the odd moments of a Gaussian distribution are zero.

Secondly, even terms only survive when the indices are fully contracted, e.g.

$$J^2_{ijkl}, \qquad J^4_{ijkl}, \qquad J^2_{ijkl} J^2_{i'j'l'l'} \tag{2.14}$$

Thirdly, because of the antisymmetry of J_{ijkl}, the fermion flavours of any lines connecting to the vertex have to be different. For example, since $J_{iikl} = 0$, it is not possible to draw a vertex with an incoming and outcoming i particle.

These rules greatly restrict the number of allowed Feynman diagrams. The full set is given in Figure 2.1.

Careful observation of these diagrams leads to the following recursive definition of the 1PI diagrams:

$$\Sigma(t_1, t_2) = J^2 G(t_1, t_2)^3 \tag{2.15}$$

$G(i\omega)$ can now be rewritten in terms of 1PI diagrams:

$$G(i\omega) = \frac{1}{i\omega} + \frac{1}{i\omega}\Sigma(i\omega)\frac{1}{i\omega} + \frac{1}{i\omega}\Sigma(i\omega)\frac{1}{i\omega}\Sigma(i\omega)\frac{1}{i\omega} + \ldots \tag{2.16}$$
$$= \frac{1}{i\omega}\sum_{n=0}^{\infty}\left(\frac{\Sigma(i\omega)}{i\omega}\right)^n = \frac{1}{i\omega}\frac{1}{1 - \left(\frac{\Sigma(i\omega)}{i\omega}\right)} \tag{2.17}$$

Therefore,

$$G(i\omega)^{-1} = i\omega - \Sigma(i\omega) \tag{2.18}$$

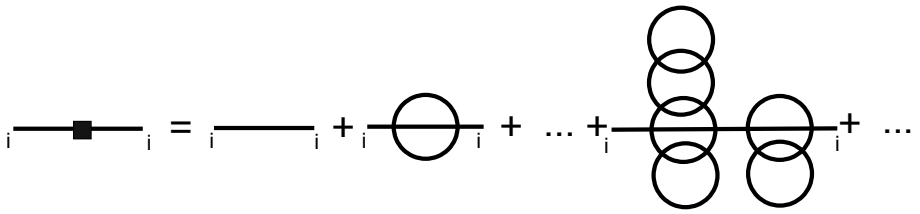

(a) The full two-point function.

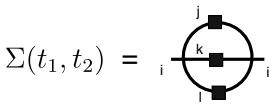

(b) Recursive definition of the 1PI diagrams.

Figure 2.1: The Feynman diagrams for the four fermion SYK model. A box indicates the full propagator. Image courtesy of [13].

To obtain $G(t_1, t_2)$, (2.18) has to be inverted. This can be done analytically when $\Sigma(i\omega) \gg i\omega$, which is in the low energy (or strongly coupled) limit.

$$\begin{aligned} \int \mathrm{d}t G(t_1, t) G(t, t_2)^{-1} &= -\delta(t_1 - t_2) \\ \int \mathrm{d}t G(t_1, t) \Sigma(t, t_2) &= -\delta(t_1 - t_2) \\ J^2 \int \mathrm{d}t G(t_1, t) G(t, t_2)^3 &= -\delta(t_1 - t_2) \end{aligned} \tag{2.19}$$

Using an ansatz of the form

$$G(t) = \frac{a}{\sqrt{|t|}} \mathrm{sgn}(t) \tag{2.20}$$

it can be checked that a solution is given by

$$G(t) = -\left(\frac{1}{4\pi J^2}\right)^{\frac{1}{4}} \frac{1}{\sqrt{|t|}} \mathrm{sgn}(t) \tag{2.21}$$

This is the zero temperature or $\beta = \infty$ solution. Going to the finite temperature solution is simplified greatly by observing that (2.19) has an emergent conformal symmetry.

2.3 Emergent Conformal Symmetry

The Schwinger-Dyson equation (2.19) has a conformal symmetry.

$$\int \mathrm{d}t G(t_1, t) \Sigma(t, t_2) = -\delta(t_1 - t_2) \tag{2.22}$$

$$J^2 \int \mathrm{d}t G(t_1, t) G(t, t_2)^3 = -\delta(t_1 - t_2) \tag{2.23}$$

These equations are invariant under the reparametrization[13]

$$G(t_1, t_2) \to |\partial_1 f(t_1)\partial_2 f(t_2)|^{1/4} G(f(t_1), f(t_2)) \tag{2.24}$$

$$\Sigma(t_1, t_2) \to |\partial_1 f(t_1)\partial_2 f(t_2)|^{3/4} \Sigma(f(t_1), f(t_2)) \tag{2.25}$$

And are therefore conformal. To get to finite temperature, choose $f(t) = e^{2\pi i t/\beta}$ to map the time axis to a circle. This maps the zero-temperature two-point function (2.21) into a finite temperature two-point function,

$$G_\beta(t) = -\frac{\pi^{1/4}}{\sqrt{2\beta J}} \frac{1}{\sqrt{\sin \pi t/\beta}} \tag{2.26}$$

However, using this mapping we ended up with imaginary time. Therefore, we analytically continue to real time by plugging in $t = -it_r$.

$$G_\beta(t_r) = \frac{\pi^{1/4}}{\sqrt{2\beta J}} \frac{1}{\sqrt{\sinh \pi t_r/\beta}} \tag{2.27}$$

This is the finite temperature result. Because of the sinh function this two-point function decays exponentially as t_r becomes large. This is to be expected for a strongly coupled CFT, since two points that are separated by a large amount of time are not expected to be correlated in a strongly interacting theory (at finite temperature).

2.4 Solvable at Strong Coupling

The above derivation of (2.27), is only valid at low energies where $i\omega$ is small, or equivalently, at strong coupling where $\Sigma(t_1, t_2)$ is large. In general, the time separation should satisfy $J|t| \gg 1$.

2.5 Four-point Function

In order to analyze the chaotic behavior in the four fermion model, the four-point function (2.28) has to be investigated.

$$\langle \chi_i(t_1)\chi_i(t_2)\chi_j(t_3)\chi_j(t_4)\rangle \tag{2.28}$$

Just like two point function in Section 2.2, the four-point function is governed by simple rules. The ladder diagrams in Figure 2.2a give the Feynman diagrams contributing to the four-point function.

Analysis of the Feynman diagrams leads to the following Schwinger-Dyson equation:

$$\Gamma(t_1, t_2, t_3, t_4) = \Gamma_0(t_1, t_2, t_3, t_4) + \int \mathrm{d}t_a \, \mathrm{d}t_b \Gamma(t_1, t_2, t_a, t_b) K(t_a, t_b, t_3, t_4) \tag{2.29}$$

with

$$K(t_a, t_b, t_3, t_4) = -3J^2 G(t_a, t_3) G(t_b, t_4) G(t_3, t_4)^2 \tag{2.30}$$

$$\Gamma_0(t_1, t_2, t_3, t_4) = 3J^2 \delta(t_1 - t_3)\delta(t_2 - t_4) G(t_1, t_2)^2 \tag{2.31}$$

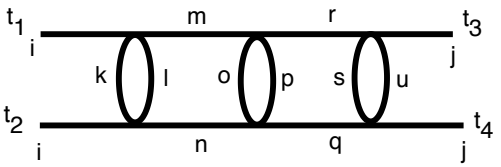

(a) The full four-point function.

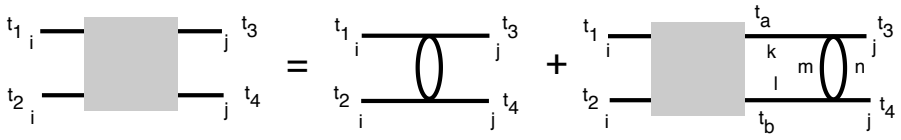

(b) Schwinger-Dyson Equation of the four-point function.

Figure 2.2: Image courtesy of [13].

This is shown pictorially in Figure 2.2b. The Schwinger-Dyson equation can be solved, and by using the conformal symmetry of the Schwinger-Dyson equation it can be shown that[13]

$$\langle \chi_i(t_1)\chi_i(t_2)\chi_j(t_3)\chi_j(t_4)\rangle_\beta \sim \frac{1}{N} e^{\lambda_L t} \tag{2.32}$$

Using (2.32), Kitaev managed to show that $\lambda_L = \frac{2\pi}{\beta}$ at strong coupling for the SYK model[9]. This is the same as for a black hole[14], making the SYK model a promising model for the study of quantum chaos.

Chapter 3

Eigenvalue Distribution

Since all the interesting physics of the SYK model is in the low energy/strong coupling limit, a natural question to ask is: what does the eigenvalue distribution look like?

A numerical simulation[10] of the $q = 4$ model with $N = 32$ is shown in Figure 3.1. It is expected that with increasing N, this will asymptotically approach a Gaussian distribution. However, all the interesting physics is encoded in the deviation from Gaussian behavior. It would therefore be very helpful if the exact distribution could be calculated.

Unfortunately, numerical simulations cannot help with this investigation into the large N limit. This is because the size of $\mathcal{H}$ scales as $\mathcal{O}(2^{\lfloor N/2 \rfloor})$, so very quickly a computer will run out of memory. Additionally, the number of matrix additions that needs to be performed is $\binom{N}{q}$, a number that grows as $\mathcal{O}(N^q)$ (For more details, see Chapter 7).

Therefore, an analytical approach is needed. In this chapter, the analytical tools needed to explore this question are explained. In Chapters 4 and 5, these techniques shall be used in an attempt to calculate the eigenvalue distribution of the one- and two-fermion model, respectively.

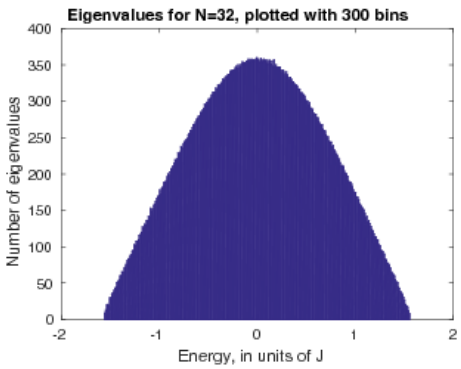

Figure 3.1: Eigenvalues for the $q = 4$ Hamiltonian with $N = 32$. Image credits: J. Maldacena, D. Stanford, [10]

3.1 Moments of the eigenvalues

Since the $J_{\mu_1\mu_2\ldots\mu_q}$ are drawn from a probability distribution, the eigenvalues ω_i of $\mathcal{H}$ will vary for every instance of $\mathcal{H}$. However, the distribution of the ω_i can be calculated by calculating the moments $\langle\omega_i^{2k}\rangle$ first, and then calculating the characteristic function from these moments (Section 3.2).

By tracing the Hamiltonian, a measure for the eigenvalues is obtained. If $\mathcal{H}$ is diagonalized as PDP^{-1}, then

$$\mathrm{tr}\left(\mathcal{H}\right) = \mathrm{tr}\left(D\right) = \sum_{i=1}^{2^{N/2}} \omega_i \tag{3.1}$$

Therefore, the even moments of the eigenvalues ω_i are obtained from $\left\langle \mathrm{tr}\left(\mathcal{H}^{2k}\right)\right\rangle$:

$$\left\langle \mathrm{tr}\left(\mathcal{H}^{2k}\right)\right\rangle = \left\langle \mathrm{tr}\left(D^{2k}\right)\right\rangle = \sum_{i=1}^{2^{N/2}} \left\langle\omega_i^{2k}\right\rangle = \left\langle\omega_i^{2k}\right\rangle \mathrm{tr}\left(\mathbb{1}\right) \tag{3.2}$$

This last step is due to the anti-commutation properties of χ_i, which ensures that the eigenvalues are always proportional to identity and therefore identically distributed. The odd moments are all zero.

3.2 Probability Density Function of the eigenvalues

The characteristic function $\phi(t)$ of a random variable is the most fundamental property of a probability distribution. If the random variable has a probability density function (pdf), then the characteristic function is the Fourier transform of the pdf.

The definition of $\phi(t)$ is given by Equation (4.16)

$$\phi(t) = \left\langle e^{it\omega}\right\rangle = \mathcal{F}\left[P(\omega)\right] = \int_{-\infty}^{\infty} e^{it\omega} P(\omega)\,\mathrm{d}\omega = \sum_{n=0}^{\infty} \frac{(it)^n}{n!}\left\langle\omega^n\right\rangle \tag{3.3}$$

The characteristic function can therefore be found from the moments by calculating $\sum_{n=0}^{\infty} \frac{(it)^n}{n!}\left\langle\omega^n\right\rangle$. Once this has been done, the pdf is obtained via inverse Fourier transform:

$$P(x) = \mathcal{F}^{-1}\left[\phi(t)\right] \tag{3.4}$$

Chapter 4

One Fermion Model

The one fermion SYK Hamiltonian is given below:

$$\mathcal{H} = \sum_{\mu=1}^{N} J_\mu \chi^\mu \tag{4.1}$$

This slightly trivial model is studied as a toy model for more complicated SYK Hamiltonians. It is well known that the sum of Gaussian distributed variables is itself Gaussian distributed. However, what happens for a sum of anti-commuting Gaussian variables?

4.1 Moments

Brute force calculation (Appendix B) shows a very clear pattern:

$$\begin{aligned}
\left\langle \mathrm{tr}\left(\mathcal{H}^2\right)\right\rangle &= N\sigma^2 \mathrm{tr}\left(\mathbb{1}\right) \\
\left\langle \mathrm{tr}\left(\mathcal{H}^4\right)\right\rangle &= N(N+2)\sigma^4 \mathrm{tr}\left(\mathbb{1}\right) \\
\left\langle \mathrm{tr}\left(\mathcal{H}^6\right)\right\rangle &= N(N+2)(N+4)\sigma^6 \mathrm{tr}\left(\mathbb{1}\right) \\
\left\langle \mathrm{tr}\left(\mathcal{H}^8\right)\right\rangle &= N(N+2)(N+4)(N+6)\sigma^8 \mathrm{tr}\left(\mathbb{1}\right)
\end{aligned}$$

Claim. $\left\langle \mathrm{tr}\left(\mathcal{H}^{2k}\right)\right\rangle = \sigma^{2k}\prod_{j=0}^{k-1}(N+2j)\mathrm{tr}\left(\mathbb{1}\right), \qquad \left\langle \omega^{2k}\right\rangle = \sigma^{2k}\prod_{j=0}^{k-1}(N+2j)$

Proof. This conjecture can be proven via induction. For the trace of gamma matrices, the following recursive definition is known: [15]

$$\mathrm{tr}\left(\chi_{\nu_1}\cdots\chi_{\nu_{2k}}\right) = \sum_{n=2}^{2k}(-1)^n \delta_{\nu_1\nu_n}\mathrm{tr}\left(\chi_{\nu_2}\cdots\cancel{\chi_{\nu_n}}\cdots\chi_{\nu_{2k}}\right) \tag{4.2}$$

Applying this to the Hamiltonian yields

$$\mathrm{tr}\left(\mathcal{H}^{2k}\right) = J_{\nu_1}J_{\nu_2}\cdots J_{\nu_{2k}}\mathrm{tr}\left(\chi_{\nu_1}\chi_{\nu_2}\cdots\chi_{\nu_{2k}}\right) \tag{4.3}$$

$$= J_{\nu_1}^2\sum_{n=2}^{2k}(-1)^n J_{\nu_2}\cdots\cancel{J_{\nu_n}}\cdots J_{\nu_{2k}}\mathrm{tr}\left(\chi_{\nu_2}\cdots\cancel{\chi_{\nu_n}}\cdots\chi_{\nu_{2k}}\right) \tag{4.4}$$

$$= J_{\nu_1}^2\sum_{n=2}^{2k}(-1)^n \mathrm{tr}\left(\mathcal{H}^{2k-2}\right) = J_{\nu_1}^2\,\mathrm{tr}\left(\mathcal{H}^{2k-2}\right) \tag{4.5}$$

The disorder average of the Hamiltonian is given by

$$\left\langle \mathrm{tr}\left(\mathcal{H}^{2k}\right)\right\rangle = \frac{1}{Z}\left(\int \prod_{j=1}^{N} \mathrm{d}J_j e^{-\frac{J_j^2}{2\sigma^2}}\right) \mathrm{tr}\left(\mathcal{H}^{2k}\right) \tag{4.6}$$

$$Z = \int \prod_{j=1}^{N} \mathrm{d}J_j e^{-\frac{J_j^2}{2\sigma^2}} = \left(\sqrt{2\pi}\sigma\right)^N \tag{4.7}$$

Combining this with (4.5), the proof follows after some careful algebraic manipulation:

$$\left\langle \mathrm{tr}\left(\mathcal{H}^{2k}\right)\right\rangle = \frac{1}{Z}\left(\int \prod_{j=1}^{N} \mathrm{d}J_j e^{-\frac{J_j^2}{2\sigma^2}}\right) J_{\nu_1}^2 \mathrm{tr}\left(\mathcal{H}^{2k-2}\right) \tag{4.8}$$

$$= \frac{1}{Z}\frac{\mathrm{d}}{\mathrm{d}(-\frac{1}{2\sigma^2})}\left[\left(\int \prod_{j=1}^{N} \mathrm{d}J_j e^{-\frac{J_j^2}{2\sigma^2}}\right) \mathrm{tr}\left(\mathcal{H}^{2k-2}\right)\right] \tag{4.9}$$

We recognize the expression inside the square brackets as $Z\left\langle \mathrm{tr}\left(\mathcal{H}^{2k-2}\right)\right\rangle$, which if the claim is right should be identical to $Z\sigma^{2k-2}\prod_{j=0}^{k-2}(N+2j)$. Therefore

$$\left\langle \mathrm{tr}\left(\mathcal{H}^{2k}\right)\right\rangle = \frac{1}{Z}\frac{\mathrm{d}}{\mathrm{d}(-\frac{1}{2\sigma^2})}\left[Z\left\langle \mathrm{tr}\left(\mathcal{H}^{2k-2}\right)\right\rangle\right] \tag{4.10}$$

$$= \frac{1}{Z}\sigma^3\frac{\mathrm{d}}{\mathrm{d}\sigma}\left[\left(\sqrt{2\pi}\sigma\right)^N \sigma^{2k-2}\prod_{j=0}^{k-2}(N+2j)\right] \tag{4.11}$$

$$= \sigma^{3-N}\frac{\mathrm{d}}{\mathrm{d}\sigma}\sigma^{N+2k-2}\prod_{j=0}^{k-2}(N+2j) \tag{4.12}$$

$$= \sigma^{2k}\prod_{j=0}^{k-1}(N+2j) \tag{4.13}$$

This completes the proof. □

For the discussion that follows this result can be rewritten in a slightly more useful form:

$$\left\langle \omega^{2k}\right\rangle = \sigma^{2k}\prod_{j=0}^{k-1}(N+2j) = \sigma^{2k}\frac{(N+2k-2)!!}{(N-2)!!} \tag{4.14}$$

$$= \sigma^{2k}2^k\frac{(\frac{N}{2}+k-1)!}{(\frac{N}{2}-1)!} = \sigma^{2k}2^k\left(\frac{N}{2}\right)^{(k)} \tag{4.15}$$

Where $x^{(n)}$ is the rising factorial. What distribution do these moments belong to?

4.2 Characteristic Function

The characteristic function of a random variable $\phi(t)$ is the most fundamental property of a probability distribution. It is defined by Equation (4.16)

$$\phi(t) = \left\langle e^{it\omega} \right\rangle = \mathcal{F}\left[P(\omega)\right] = \int_{-\infty}^{\infty} e^{it\omega} P(\omega)\,\mathrm{d}\omega = \sum_{n=0}^{\infty} \frac{(it)^n}{n!} \left\langle \omega^n \right\rangle \tag{4.16}$$

In case of the one fermion model this becomes

$$\phi(t) = \sum_{n=0}^{\infty} \frac{(it)^n}{n!} \left\langle \omega^n \right\rangle = \sum_{n \text{ even}} \frac{(it)^n}{n!} \sigma^n 2^{n/2} \left(\frac{N}{2}\right)^{(n/2)} \tag{4.17}$$

$$= \sum_{k=0}^{\infty} \frac{(it)^{2k}}{(2k)!} \sigma^{2k} 2^k \left(\frac{N}{2}\right)^{(k)} = \sum_{k=0}^{\infty} (-\frac{1}{2} t^2 \sigma^2)^k \frac{2^{2k}}{(2k)!} \left(\frac{N}{2}\right)^{(k)} \tag{4.18}$$

$$= \sum_{k=0}^{\infty} \frac{(-\frac{1}{2} t^2 \sigma^2)^k}{k!} \frac{\left(\frac{N}{2}\right)^{(k)}}{\left(\frac{1}{2}\right)^{(k)}} = {}_1F_1\left(\frac{N}{2}, \frac{1}{2}; -\frac{1}{2} t^2 \sigma^2\right) \tag{4.19}$$

The characteristic function is a confluent hypergeometric function.

4.3 Moment Generating Function

The moment generating function M is obtained by performing a Wick rotation on the characteristic function. This means that $M(t) = \phi(-it)$.

$$M(t) = \phi(-it) = {}_1F_1\left(\frac{N}{2}, \frac{1}{2}; \frac{1}{2} t^2 \sigma^2\right) \tag{4.20}$$

4.4 Probability Density Function

The Probability Density Function (pdf) is obtained from the characteristic function by performing an inverse Fourier transform:

$$P(\omega) = \mathcal{F}^{-1}\left[\phi(t)\right] = \mathcal{F}^{-1}\left[{}_1F_1\left(\frac{N}{2}, \frac{1}{2}; -\frac{1}{2} t^2 \sigma^2\right)\right] \tag{4.21}$$

$$= \frac{1}{\Gamma\left(\frac{N}{2}\right)} \left(\frac{1}{2\sigma^2}\right)^{\frac{N}{2}} |\omega|^{-1+N} \exp\left[-\frac{\omega^2}{2\sigma^2}\right] \tag{4.22}$$

Plugging in $N = 1$ we find that we get back the normal Gaussian pdf, as expected. However, for larger N a clear deviation from Gaussian is expected because of the $|\omega|$

4.5 Numerical Validation

Numerical simulations have been perform to confirm this distribution.

In Figure 4.1 the numerical simulation and the calculated distribution for $N = 2$ have been plotted. It can be seen that the two are in excellent agreement.

In Figure 4.2 the same has been done for $N = 16$. Also here the two are in excellent agreement. The slightly larger deviations from the prediction as compared to the $N = 2$ case, can be attributed to the smaller sample size used. This is due to the computational complexity growing as $\mathcal{O}(2^N)$.

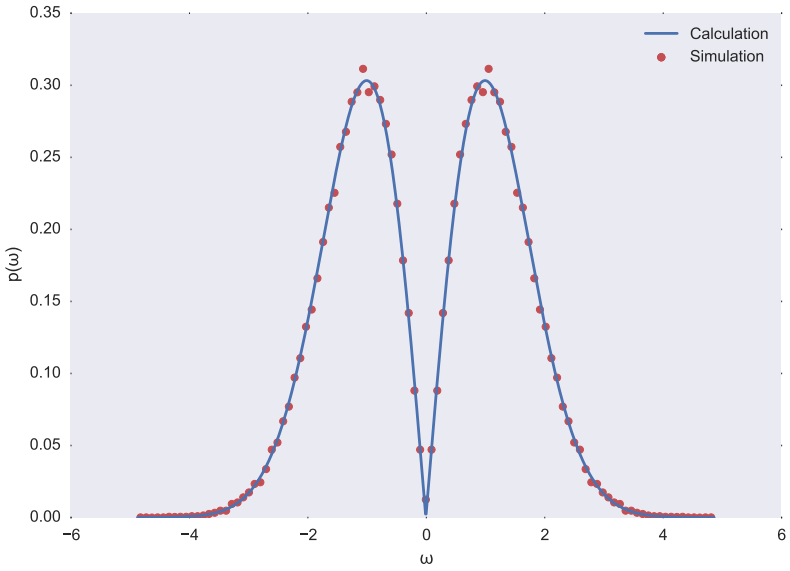

Figure 4.1: Numerical simulation for $N = 2$, 10^5 samples.

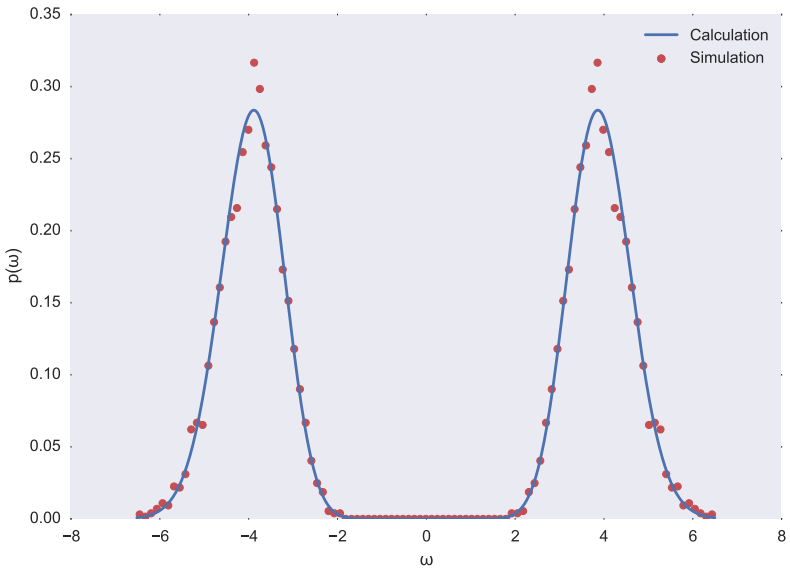

Figure 4.2: Numerical simulation for $N = 16$, 10^4 samples.

Chapter 5

Two Fermion Model

The two fermion SYK Hamiltonian is given below:

$$\mathcal{H} = i \sum_{\mu>\nu} J_{\mu\nu} \chi^{\mu} \chi^{\nu} = \frac{i}{2} \sum_{\mu,\nu} J_{\mu\nu} \chi^{\mu\nu} \tag{5.1}$$

In this form the Hamiltonian looks very similar to the one fermion case. When proofing the moments for the one fermion case the recursive definition of the trace was crucial. After calculating the equivalent for the two fermion case an attempt can be made to calculate the moments for the two fermion model.

A brute force calculation (Appendix B) yields

$$\left\langle \mathrm{tr}\left(\mathcal{H}^2\right)\right\rangle = \binom{N}{2} \sigma^2 \mathrm{tr}\left(\mathbb{1}\right) \tag{5.2}$$

$$\left\langle \mathrm{tr}\left(\mathcal{H}^4\right)\right\rangle = 3\left[\binom{N}{2} + 2\binom{N}{3} + 6\binom{N}{4}\right] \sigma^4 \mathrm{tr}\left(\mathbb{1}\right) \tag{5.3}$$

5.1 Recursive Definition of the Trace

In the *one fermion* model the recursive definition (5.4) of the trace is at the center of the computation.

$$\mathrm{tr}\left(\chi_{\nu_1} \cdots \chi_{\nu_{2k}}\right) = \sum_{n=2}^{2k} (-1)^n \delta_{\nu_1\nu_n} \mathrm{tr}\left(\chi_{\nu_2} \cdots \cancel{\chi_{\nu_n}} \cdots \chi_{\nu_{2k}}\right) \tag{5.4}$$

This well known result can be derived using $\mathrm{tr}\left(AB\right) = \mathrm{tr}\left(BA\right) = \frac{1}{2}\mathrm{tr}\left(\{A,B\}\right)$ and $\{\chi_\mu, \chi_\nu\} = 2\delta_{\mu\nu}$, and by applying this to $\frac{1}{2}\mathrm{tr}\left(\{\chi_{\nu_1}, \chi_{\nu_2} \cdots \chi_{\nu_{2k}}\}\right)$.

The same process can be applied to the two-fermion case.

Claim. $\{\chi^{\mu\nu}, \chi^{\rho\sigma}\} = 2\chi^{\mu\nu\rho\sigma} + 4\delta^{[\mu}_{[\sigma}\delta^{\nu]}_{\rho]}$

To understand this commutator, and indeed this chapter, it is recommended to read Appendix A.

$$\begin{aligned}\mathrm{tr}\left(\chi_{\mu_1\nu_1}\cdots\chi_{\mu_{2k}\nu_{2k}}\right) =&\frac{1}{2}\sum_{n=2}^{2k}(-1)^n\mathrm{tr}\left(\chi_{\mu_2\nu_2}\cdots\{\chi_{\mu_1\nu_1},\chi_{\mu_n\nu_n}\}\cdots\chi_{\mu_{2k}\nu_{2k}}\right)\\ =&2\sum_{n=2}^{2k}(-1)^n\delta^{[\mu_1}_{[\nu_n}\delta^{\nu_1]}_{\mu_n]}\mathrm{tr}\left(\chi_{\mu_2\nu_2}\cdots\cancel{\chi_{\mu_n\nu_n}}\cdots\chi_{\mu_{2k}\nu_{2k}}\right)\\ &+\sum_{n=2}^{2k}(-1)^n\mathrm{tr}\left(\chi_{\mu_1\nu_1\mu_n\nu_n}\chi_{\mu_{n+1}\nu_{n+1}}\cdots\chi_{\mu_{2k}\nu_{2k}}\chi_{\mu_2\nu_2}\cdots\chi_{\mu_{n-1}\nu_{n-1}}\right)\end{aligned} \tag{5.5}$$

Applying this to the Hamiltonian gives

$$\begin{aligned}\mathrm{tr}\left(\mathcal{H}^{2k}\right) =&\frac{2}{4}J^2_{\mu_1\nu_1}\mathrm{tr}\left(\mathcal{H}^{2k-2}\right)\\ &+\frac{1}{4}J_{\mu_1\nu_1}J_{\mu_2\nu_2}\mathrm{tr}\left(\chi_{\mu_1\nu_1\mu_2\nu_2}\mathcal{H}^{2k-2}\right)\end{aligned} \tag{5.6}$$

The appearance of the second term means that in general this does not lead to a simple recursive definition of $\mathrm{tr}\left(\mathcal{H}^{2k}\right)$. However, it can be observed that since for $N<4$, $\chi_{\mu_1\nu_1\mu_2\nu_2}=0$, the one-fermion behavior is recovered for $2\leq N<4$, and the two fermion model is distributed as the one fermion model with $N\to\binom{N}{2}$. This is shown in Figure 5.1 for $N=2$ and $N=3$. When N is increased beyond this, $\chi_{\mu_1\nu_1\mu_2\nu_2}$ is no longer zero so the behavior is no longer simple. More simulations of this behavior are given in Chapter 7.

Corollary 5.1.0.1. *For the general q fermion model, the $q\leq N<q+2$ case is distributed like the one fermion model with $\binom{N}{q}$ fermions.*

In general then, this approach does not yield a closed expression for the moments of the two fermion model. However, Corollary 5.1.0.1 does offer an interesting insight; if the large N model with $q=N-1$ is still chaotic, we have an exact discription of its eigenvalue distribution.

5.2 Wigner semicircle

In their paper "Comments on the SYK" model, J. Maldacena and D. Stanford comment that in the $\chi_\mu\chi_\nu$ basis, the matrix $J_{\mu\nu}$ has a Wigner semicircle distribution in the large N limit. Indeed, any (anti-)Hermitian $N\times N$ matrix assymptotically approaches a Wigner semicircle distribution in the large N limit[16].

In traditional proofs, one defines a Hermitian Gaussian random matrix H_N by letting

$$\langle x|H_N|y\rangle=\begin{cases}\mathcal{N}\left(0,v^2\right)_{\mathbb{C}} & \text{if } x\neq y\\ \mathcal{N}\left(0,v^2\right)_{\mathbb{R}} & \text{if } x=y\end{cases} \tag{5.7}$$

One then defines the normalized eigenvalue counting function (NCF) of the Hermitian matrix H_N

$$\sigma(\lambda,H_N)=\frac{1}{N}\#\left\{\lambda_j\leq\lambda\right\} \tag{5.8}$$

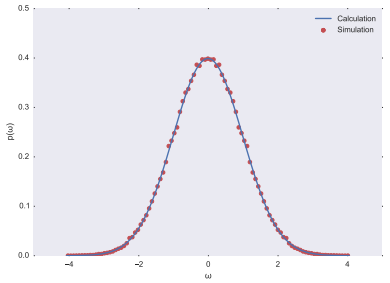

(a) $N = 2$, 10^6 samples.

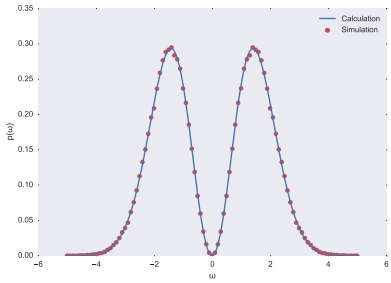

(b) $N = 3$, 10^6 samples.

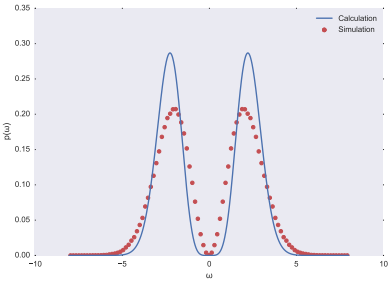

(c) $N = 4$, 10^6 samples.

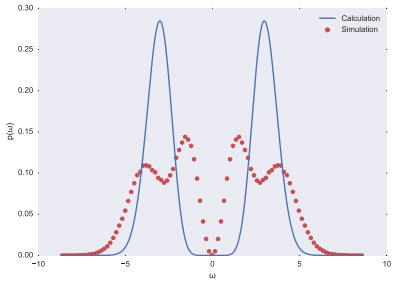

(d) $N = 5$, 10^6 samples.

Figure 5.1: Numerical simulation of the two fermion Hamiltonian with $\sigma = 1$ for $2 \leq N < 6$.

where $\lambda_1 \leq \cdots \leq \lambda_N$ are the eigenvalues of H_N. This simply counts the number of eigenvalues less or equal to λ. It can then be shown that for large N, this weakly converges in average to the Wigner semicircle distribution:

$$\sigma_W(\lambda) = \sqrt{4v^2 - \lambda^2} \tag{5.9}$$

However, in this section a more intuitive approach is given. Firstly, let's rewrite the Hamiltonian in matrix notation:

$$\mathcal{H} = \frac{i}{2} J_{\mu\nu} \chi_\mu \chi_\nu = \frac{i}{2} \boldsymbol{\chi}^\dagger \boldsymbol{J} \boldsymbol{\chi} \tag{5.10}$$

We now rewrite $\boldsymbol{J}$ as an Hermitian operator $\hat{J} = i\boldsymbol{J}$ in braket notation:

$$\hat{J} = i\boldsymbol{J} = i \sum_{\mu\nu} J_{\mu\nu} \left|\mu\right\rangle \left\langle\nu\right| \tag{5.11}$$

$$\boldsymbol{\chi} = \sum_{\mu} \left|\mu\right\rangle \chi_\mu \tag{5.12}$$

It is easy to check that $\hat{J}$ is an Hermitian operator, which will make calculating the eigenvalue distribution easier than working with an anti-symmetric operator. Let us denote the trace of an operator $\hat{A}$ in this basis as $\operatorname{tr}_\chi \hat{A}$.

Calculating the moments of the eigenvalues of $\hat{J}$ now becomes particularly easy:

$$\begin{aligned}
\operatorname{tr}_\chi \hat{J}^2 &= i^2 \sum_n \left\langle n\right| \sum_{\mu\nu} J_{\mu\nu} \left|\mu\right\rangle \left\langle\nu\right| \sum_{\rho\sigma} J_{\rho\sigma} \left|\rho\right\rangle \left\langle\sigma|n\right\rangle \\
&= - \sum_{n\mu\nu\rho\sigma} J_{\mu\nu} J_{\rho\sigma} \left\langle n|\mu\right\rangle \left\langle\nu|\rho\right\rangle \left\langle\sigma|n\right\rangle \\
&= - \sum_{\mu\nu} J_{\mu\nu} J_{\nu\mu} \\
\operatorname{tr}_\chi \hat{J}^2 &= \sum_{\mu\nu} J_{\mu\nu}^2
\end{aligned}$$

Similarly,

$$\begin{aligned}
\operatorname{tr}_\chi \hat{J}^4 &= \sum_{\mu\nu\rho\sigma} J_{\mu\nu} J_{\nu\rho} J_{\rho\sigma} J_{\sigma\mu} \\
\operatorname{tr}_\chi \hat{J}^6 &= - \sum_{\mu\nu\rho\sigma\lambda\tau} J_{\mu\nu} J_{\nu\rho} J_{\rho\sigma} J_{\sigma\lambda} J_{\lambda\tau} J_{\tau\mu}
\end{aligned}$$

Generalizing to $\operatorname{tr}_\chi \hat{J}^{2k}$, this becomes

$$\operatorname{tr}_\chi \hat{J}^{2k} = i^{2k} \sum_{\mu_1\nu_1\ldots\mu_k\nu_k} J_{\mu_1\nu_1} J_{\nu_1\mu_2} J_{\mu_2\nu_2} \ldots J_{\mu_k\nu_k} J_{\nu_k\mu_1}$$

Analyzing this carefully, we see that all the $J_{\mu\nu}$ have been chained together and form a circle. This chaining is show in Figure 5.2 for increasing k.

Because of this chaining together, the number of allowed configurations is limited. In order for a contribution to be non-zero, the $J_{\mu\nu}$ have to be paired since only even moments survive.

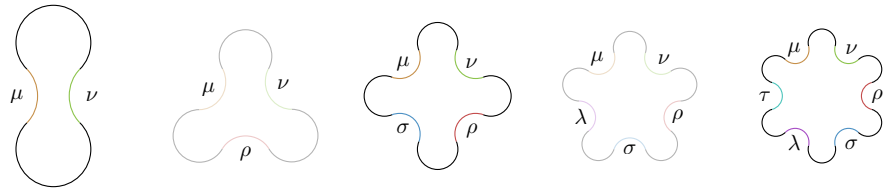

Figure 5.2: The $J_{\mu\nu}$ become chained together. Terms with an odd number of indices become zero due to Gaussian averaging and the anti-symmetry of $J_{\mu\nu}$.

Definition 5.2.1. Pair – A pair is defined as $J_{\mu\nu}J_{\nu\mu}$. This definition respects the proper chaining of the $J_{\mu\nu}$, as opposed to $J_{\mu\nu}^2$

Taking $\mathrm{tr}_\chi\, \hat{J}^6$ as an example, one possible pairing would be $\rho = \lambda = \mu$.

$$\begin{aligned}\mathrm{tr}_\chi\, \hat{J}^6 &= -\sum_{\mu\nu\rho\sigma\lambda\tau} (J_{\mu\nu}J_{\nu\rho})(J_{\rho\sigma}J_{\sigma\lambda})(J_{\lambda\tau}J_{\tau\mu}) \\ &\propto -\sum_{\mu\nu\sigma\tau} J_{\mu\nu}J_{\nu\mu}J_{\mu\sigma}J_{\sigma\mu}J_{\mu\tau}J_{\tau\mu} = \sum_{\mu\nu\sigma\tau} J_{\mu\nu}^2 J_{\mu\sigma}^2 J_{\mu\tau}^2\end{aligned}$$

Recalling that $\left\langle J_{\mu\nu}^2 \right\rangle = \sigma^2 = J^2/N$ for the $q = 2$ model, and observing that there are four indices left to sum over,

$$\left\langle \mathrm{tr}_\chi\, \hat{J}^6 \right\rangle \sim\ N^4\sigma^6 = NJ^6 \text{ as } N \gg 1$$

At large N, the terms with the highest number of indices will dominate. How many other pairings of $\mathcal{O}(N)$ in J are allowed? All $(2k-1)!!$ options for $k = 3$ are shown in Figure 5.3. From the chained expression, it is easy to convince oneself that pairing with a $J_{\mu\nu}$ an odd number of steps away results in $J_{\mu\mu} = 0$. This is illustrated in Figure 5.3 by two lines of the same color connecting to a $J_{\mu\nu}$. To convince oneself that a crossing pairing with every pairing an even number of terms away (upper right corner of Figure 5.3) is not of $\mathcal{O}(N)$, it is helpful to write out a sequence of $J_{\mu\nu}$ and to do those contractions:

$$J_{\mu\nu}J_{\nu\rho}J_{\rho\sigma}J_{\sigma\lambda}J_{\lambda\tau}J_{\tau\mu} \Rightarrow J_{\mu\nu}J_{\nu\mu}J_{\mu\nu}J_{\nu\mu}J_{\mu\nu}J_{\nu\mu} \tag{5.13}$$

The chaining forces such terms to be of lower order, $\mathcal{O}(N^{-1})$ in this example. This is illustrated in the upper right corner of Figure 5.3.

Therefore, the only pairings that survive at $\mathcal{O}(N)$ are the non-crossing ones. The number of non-crossing pairs one can form from $2k$ objects is given by the Catalan number C_k[17]:

$$C_k = \frac{1}{k+1}\binom{2k}{k} \tag{5.14}$$

This means that at large N, we are left with the expression

$$\left\langle \mathrm{tr}_\chi\, \hat{J}^6 \right\rangle = C_3 NJ^6 \text{ as } N \gg 1 \tag{5.15}$$

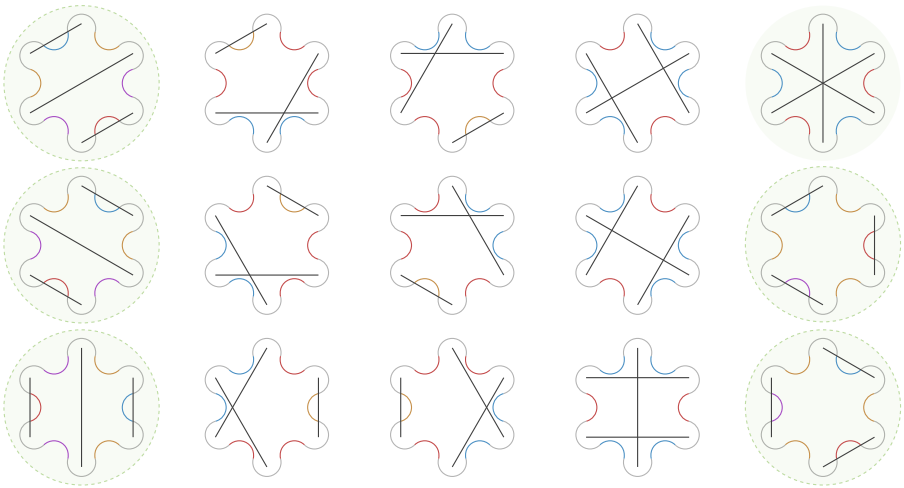

Figure 5.3: The fifteen *perfect matchings* for six objects. All the non-zero diagrams are indicated by their shaded background. The others are zero because they contain $J_{\mu\mu}$ terms, indicated by two lines of the same color connecting to a $J_{\mu\nu}$ upon pairing. Only the five non-crossing diagrams are of $\mathcal{O}(N)$. These are the diagrams encircled by a dotted line. Subleading is the fully crossing diagram in the upper right.

and for general k:

$$\mathrm{tr}_\chi\, \hat{J}^{2k} = i^{2k} C_k \sum_{\mu\nu_1\nu_2\ldots\nu_k} J_{\mu\nu_1} J_{\nu_1\mu} J_{\mu\nu_2} \ldots J_{\mu\nu_k} J_{\nu_k\mu}$$

$$\left\langle \mathrm{tr}_\chi\, \hat{J}^{2k} \right\rangle = C_k N J^{2k} \text{ as } N \gg 1 \tag{5.16}$$

The characteristic function is then given by

$$\begin{aligned}\phi(t) &= \sum_{n=0}^{\infty} \frac{(it)^n}{n!} \left\langle \mathrm{tr}_\chi\, \hat{J} \right\rangle = N \sum_{k=0}^{\infty} \frac{(itJ)^{2k}}{(2k)!} C_k \\ &= 2N \frac{J_1(Rt)}{Rt}\end{aligned}$$

where $R^2 := 4J^2$, and $J_n(z)$ denotes the Bessel function of the first kind.

Inversely Fourier transforming $\phi(t)$, the p.d.f. $P(x)$ is obtained.

$$P(x) = \frac{1}{N} \mathcal{F}^{-1}\left[\phi(t)\right] = \frac{2}{\pi R^2} \sqrt{R^2 - x^2} \quad \theta\left[-4\pi^2\left(x^2 - R^2\right)\right] \tag{5.17}$$

where $\theta\left[-4\pi^2\left(x^2 - R^2\right)\right]$ is the Heaviside step function, and the $1/N$ is introduced for normalization. We recognize this result as the Wigner semicircle distribution, which indeed is only valid for $-R \leq x \leq R$, as dictated by the Heaviside step function.

This confirms that in the $\chi_\mu\chi_\nu$ basis, the eigenvalues of $J_{\mu\nu}$ follow a Wigner semicircle distribution.

Chapter 6

Four Fermion Model

The four fermion SYK Hamiltonian is given below:

$$\mathcal{H} = \sum_{\mu>\nu>\rho>\sigma} J_{\mu\nu\rho\sigma}\chi^{\mu}\chi^{\nu}\chi^{\rho}\chi^{\sigma} = \frac{1}{4!}\sum_{\mu,\nu,\rho,\sigma} J_{\mu\nu\rho\sigma}\chi^{\mu\nu\rho\sigma} \tag{6.1}$$

Similar to the two fermion case, this form of the Hamiltonian looks very familiar to the one fermion case.

A brute force calculation (Appendix B) yields

$$\left\langle \mathrm{tr}\left(\mathcal{H}^2\right)\right\rangle = \sigma^2\binom{N}{4}\mathrm{tr}\left(\mathbb{1}\right) \tag{6.2}$$

$$\left\langle \mathrm{tr}\left(\mathcal{H}^4\right)\right\rangle \to 3\sigma^4\binom{N}{4}^2\mathrm{tr}\left(\mathbb{1}\right) \tag{6.3}$$

6.1 Recursive Definition of the Trace

Claim.

$$\begin{aligned}\{\chi^{\mu_1\nu_1\rho_1\sigma_1},\chi^{\mu_2\nu_2\rho_2\sigma_2}\} =& 2\chi^{\mu_1\nu_1\rho_1\sigma_1\mu_2\nu_2\rho_2\sigma_2} + 2C_2^{4,4}\chi^{[\mu_1\nu_1\rho_2\sigma_2}\delta^{\sigma_1}_{[\mu_2}\delta^{\rho_1]}_{\nu_2]} \\ &+ 2C_4^{4,4}\delta^{[\sigma_1}_{[\mu_2}\delta^{\rho_1}_{\nu_2}\delta^{\nu_1}_{\rho_2}\delta^{\mu_1]}_{\sigma_2]}\end{aligned}$$

The coefficients $C_r^{p,q} = r!\binom{p}{r}\binom{q}{r}$ give the number of ways r indices between an object of rank p and an object of rank q can be contracted.

In order to keep the notation clean in the discussion below, we define $(n) \coloneqq \mu_n\nu_n\rho_n\sigma_n$ such that $\chi_{(n)} = \chi_{\mu_n\nu_n\rho_n\sigma_n}$.

$$\begin{aligned}
\mathrm{tr}\left(\chi_{(1)}\cdots\chi_{(2k)}\right) &= \frac{1}{2}\sum_{n=2}^{2k}(-1)^n \mathrm{tr}\left(\chi_{(2)}\cdots\left\{\chi_{(1)},\chi_{(n)}\right\}\cdots\chi_{(2k)}\right)\\
=&4!\sum_{n=2}^{2k}(-1)^n\delta^{[\sigma_1}_{[\mu_n}\delta^{\rho_1}_{\nu_n}\delta^{\nu_1}_{\rho_n}\delta^{\mu_1]}_{\sigma_n]}\mathrm{tr}\left(\chi_{(2)}\cdots\cancel{\chi_{(n)}}\cdots\chi_{(2k)}\right)\\
&+72\sum_{n=2}^{2k}(-1)^n\mathrm{tr}\left(\chi^{[\mu_1\nu_1\rho_n\sigma_n}\delta^{\sigma_1}_{[\mu_n}\delta^{\rho_1]}_{\nu_n]}\chi_{(2)}\cdots\cancel{\chi_{(n)}}\cdots\chi_{(2k)}\right)\\
&+\sum_{n=2}^{2k}(-1)^n\mathrm{tr}\left(\chi_{\mu_1\nu_1\rho_1\sigma_1\mu_n\nu_n\rho_n\sigma_n}\chi_{(n+1)}\cdots\chi_{(2k)}\chi_{(2)}\cdots\chi_{(n-1)}\right) \qquad (6.4)
\end{aligned}$$

Applying this to the Hamiltonian gives

$$\begin{aligned}
\mathrm{tr}\left(\mathcal{H}^{2k}\right) =&\frac{4!}{(4!)^2}J^2_{\mu_1\nu_1\rho_1\sigma_1}\mathrm{tr}\left(\mathcal{H}^{2k-2}\right)\\
&+\frac{72}{(4!)^2}J_{\mu_1\nu_1\nu_2\mu_2}J_{\mu_2\nu_2\rho_2\sigma_2}\mathrm{tr}\left(\chi_{\mu_1\nu_1\rho_2\sigma_2}\mathcal{H}^{2k-2}\right)\\
&+\frac{1}{(4!)^2}J_{\mu_1\nu_1\rho_1\sigma_1}J_{\mu_2\nu_2\rho_2\sigma_2}\mathrm{tr}\left(\chi_{\mu_1\nu_1\rho_1\sigma_1\mu_2\nu_2\rho_2\sigma_2}\mathcal{H}^{2k-2}\right) \qquad (6.5)
\end{aligned}$$

Similar to the $q = 2$ Hamiltonian, this does not lead to a closed expression of $\mathrm{tr}\left(\mathcal{H}^{2k}\right)$. However, since the second term will only contribute when $N = 6$, and the third term only when $N = 8$, the one-fermion behavior is recovered for $4 \leq N < 6$. This confirms that the $q = 4$ model is distributed as the one fermion model with $N \to \binom{N}{4}$ as predicted by Corollary 5.1.0.1. Some plots of this behavior are shown in Figure 6.1. More simulations of this behavior are given in Chapter 7.

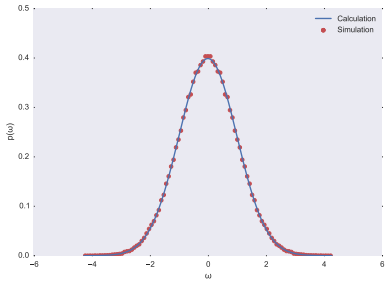

(a) $N = 4$, 10^5 samples.

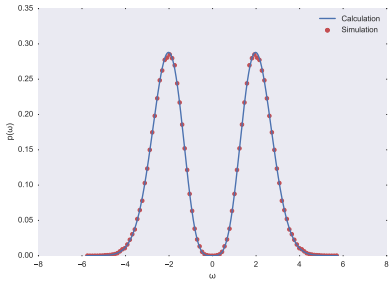

(b) $N = 5$, 10^5 samples.

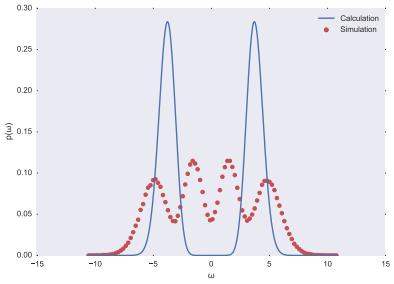

(c) $N = 6$, 510^4 samples.

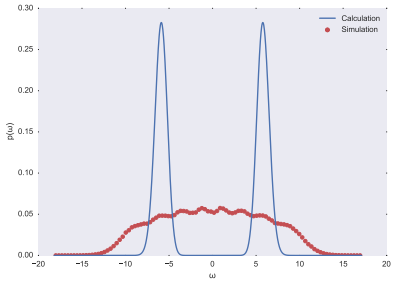

(d) $N = 7$, 510^4 samples.

Figure 6.1: Numerical simulation of the four fermion Hamiltonian with $\sigma = 1$ for $4 \leq N < 8$.

Chapter 7

Numerical Calculations

In order to verify analytical results, numerical calculations were performed. The large N limit is where the interesting physics is. However, since the γ matrices are $2^{N/2} \times 2^{N/2}$, computations for large N quickly become impossible. Methods that optimize such computations are therefore needed.

By observing how the γ matrices are generated, a method can be found to greatly speed up multiplication. The generating (Euclidean) γ matrices are built up from Kronecker products of Pauli matrices:

$$\begin{aligned}
\gamma^1 &= \sigma_1 \otimes \mathbb{1} \otimes \mathbb{1} \otimes \dots \\
\gamma^2 &= \sigma_2 \otimes \mathbb{1} \otimes \mathbb{1} \otimes \dots \\
\gamma^3 &= \sigma_3 \otimes \sigma_1 \otimes \mathbb{1} \otimes \dots \\
\gamma^4 &= \sigma_3 \otimes \sigma_2 \otimes \mathbb{1} \otimes \dots \\
\gamma^5 &= \sigma_3 \otimes \sigma_3 \otimes \sigma_1 \otimes \dots
\end{aligned}$$

But multiplication of direct product matrices can be done blockwise:

$$(A \otimes B)(C \otimes D) = (AC \otimes BD) \tag{7.1}$$

Therefore, in order to compute $\gamma^\mu \gamma^\nu$, the full matrices are not needed. Only the individual blocks have to be multiplied. This reduces the computational complexity of multiplying such matrices from the normal $\mathcal{O}(2^N)$ to $\mathcal{O}(N)$.

Despite this improvement, the large N limit remains illusive. This is because of two reasons:

- In order to perform addition the full $2^{N/2} \times 2^{N/2}$ matrix $\chi_{\mu_1}\chi_{\mu_2}\cdots\chi_{\mu_q}$ has to be computed and added for every term. There is no way to optimize addition like has been done for multiplication.
- The number of terms that have to be added grows as $\binom{N}{q} \to \mathcal{O}(N^q)$ for large N.

This means that without a supercomputer, one is still limited to $N \sim 20$.

7.1 Demonstrating Corollary 5.1.0.1

Corollary 5.1.0.1 states that *For the general q fermion model, the $q \leq N < q+2$ case is distributed like the one fermion model with $\binom{N}{q}$ fermions.*

Firstly, the deviation from the one-fermion model is shown for the $q = 2$ and $q = 4$ models in Figures 7.1 and 7.2, resp. The deviation from the one-fermion model as N increases is made very clear by these simulations.

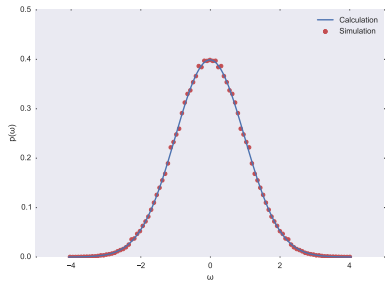

(a) $N = 2$, 10^6 samples.

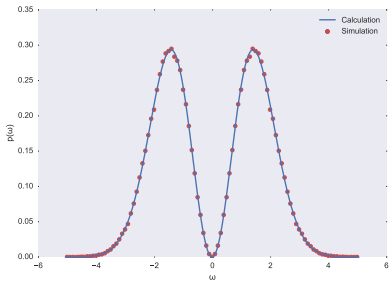

(b) $N = 3$, 10^6 samples.

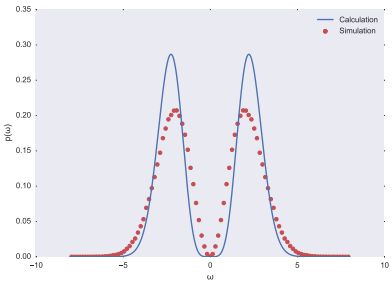

(c) $N = 4$, 10^6 samples.

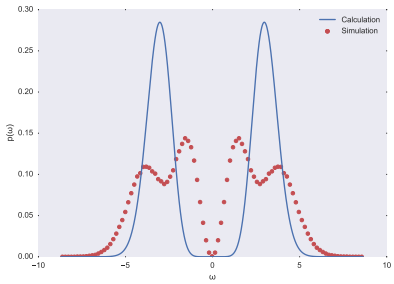

(d) $N = 5$, 10^6 samples.

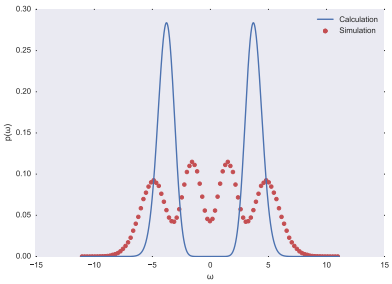

(e) $N = 6$, $5 \cdot 10^5$ samples.

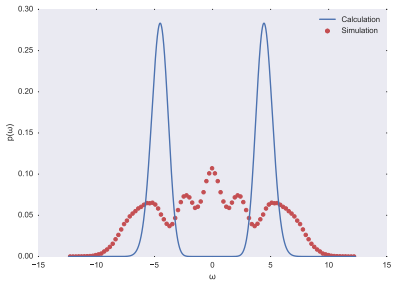

(f) $N = 7$, $5 \cdot 10^5$ samples.

Figure 7.1: Numerical simulation of the two fermion Hamiltonian with $\sigma = 1$ for $2 \leq N < 8$.

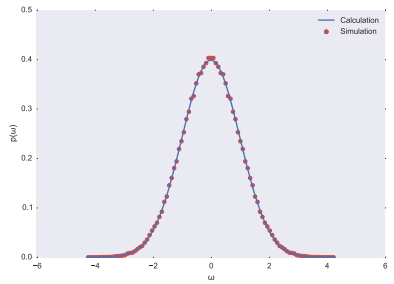

(a) $N = 4$, 10^6 samples.

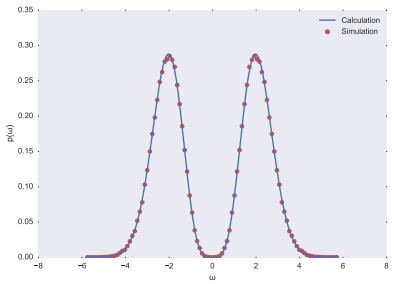

(b) $N = 5$, 10^6 samples.

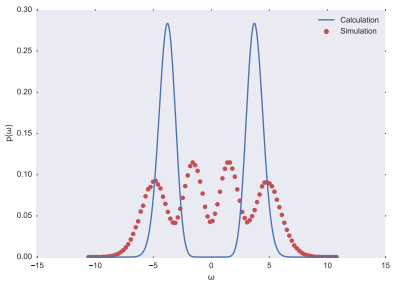

(c) $N = 6$, $5 \cdot 10^5$ samples.

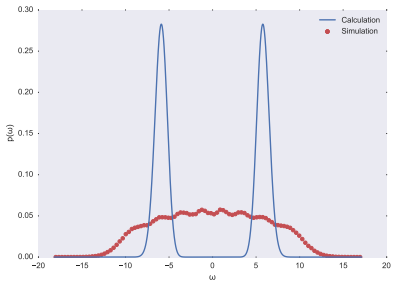

(d) $N = 7$, $5 \cdot 10^5$ samples.

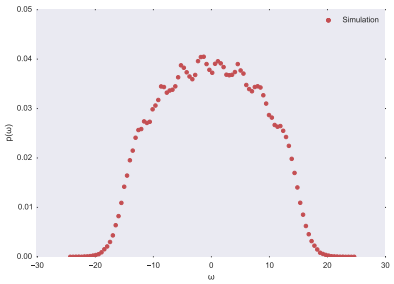

(e) $N = 8$, $2.5 \cdot 10^5$ samples.

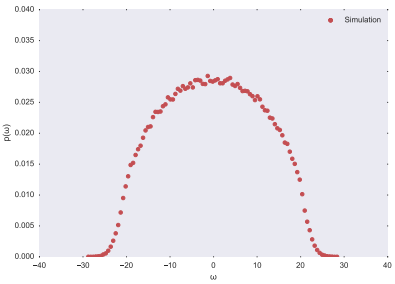

(f) $N = 9$, $2.5 \cdot 10^5$ samples.

Figure 7.2: Numerical simulation of the four fermion Hamiltonian with $\sigma = 1$ for $4 \leq N < 10$.

The opposite is demonstrated in Figure 7.3. Here both N and q are raised in such a way that $N = q + 1$. In this case, the eigenvalue distribution is given by the one fermion model.

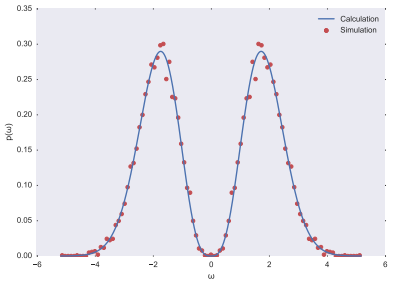

(a) $N = 4$, $q = 3$, 10^4 samples.

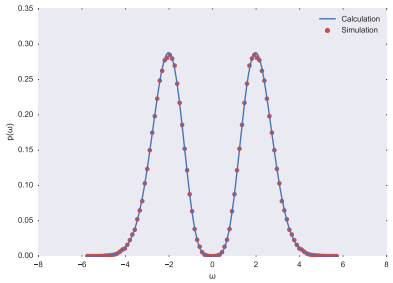

(b) $N = 5$, $q = 4$, 10^5 samples.

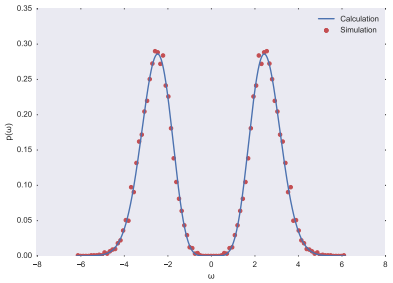

(c) $N = 7$, $q = 6$, 10^4 samples.

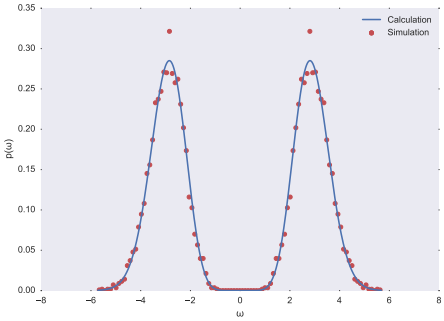

(d) $N = 9$, $q = 8$, 10^4 samples.

Figure 7.3: Numerical simulation of ever increasing $N = q + 1$.

Chapter 8

Discussion and Conclusion

The one fermion model was solved entirely. As a purely mathematical toy model, a lot could be learned from it. Additionally, it describes the $q \leq N < q+1$ behavior of general q models.

Studying the one fermion model shaped this thesis in a number of ways. Firstly, it outlines the procedure needed to get from the moments of a distribution to the probability density function. Secondly, it suggests that the method of finding a recursive definition of the trace could also work for general q models. Lastly, it lead to Corollary 5.1.0.1, which is perhaps the most promising result of this thesis.

It states that for $q \leq N < q+2$ the q fermion model follows the one fermion distribution. The $N = q$ case is probably not chaotic, but the $N = q+1$ case might still be chaotic. This is worth investigating, since we would know exactly what the spectrum of the model is, and therefore what the possible groundstates of the theory are.

In investigating the two fermion model, it was found that although it is possible to find a recursive definition of the trace over gamma matrices for any q, this does not result in a closed expression for the moments of q fermion SYK Hamiltonian. Therefore no eigenvalue distribution of the two fermion SYK Hamiltonian could be given. However, in the $\chi_\mu \chi_\nu$ basis the Wigner semi-circle distribution follows intuitively.

The method used to derive the Wigner semi-circle for the anti-symmetric $J_{\mu\nu}$ might be extendable to general (anti)hermitian matrices, which would provide an intuitive derivation of this distribution, which can serve as a nice complement to the typical technical derivation of this distribution.

Additionally, using the trace orthogonality of the $\chi_\mu \chi_\nu$, it should be possible to repeat the argument made for the $q = 2$ model in deriving the Wigner semi-circle distribution for the $q = 4$ model. This can be done by defining an inner product $\langle \mu, \nu | \rho, \sigma \rangle = \mathrm{tr}\left(\chi_{\mu\nu}\chi_{\rho\sigma}\right)$ and then repeating the logic.

8.1 Acknowledgements

I would like to thank prof. Kyriakos Papadodimas for allowing me to work in his group, and for the extremely interesting conversations we have had. Additionally I would like to thank Randy Wind for creating Figures 5.2 and 5.3.

Appendices

Appendix A

Clifford Algebras and anti-symmetric products.

This appendix summerizes the most important properties of the Dirac γ-matrices as used in this thesis. These matrices form the generating elements of a Clifford Algebra. Most of the methods described here are taken from [11], complemented by [12], and [15].

Most importantly for this thesis, the properties of anti-symmetric products are described.

A.1 Generating γ-matrices

The generating (Euclidean) γ-matrices are defined by their anti-commutation relations:

$$\{\gamma^\mu, \gamma^\nu\} = 2g^{\mu\nu} = 2\delta^{\mu\nu} \tag{A.1}$$

These matrices can be constructed explicitly by taking Kronecker products of Pauli-matrices:

$$\begin{aligned}
\gamma^1 &= \sigma_1 \otimes \mathbb{1} \otimes \mathbb{1} \otimes \dots \\
\gamma^2 &= \sigma_2 \otimes \mathbb{1} \otimes \mathbb{1} \otimes \dots \\
\gamma^3 &= \sigma_3 \otimes \sigma_1 \otimes \mathbb{1} \otimes \dots \\
\gamma^4 &= \sigma_3 \otimes \sigma_2 \otimes \mathbb{1} \otimes \dots \\
\gamma^5 &= \sigma_3 \otimes \sigma_3 \otimes \sigma_1 \otimes \dots
\end{aligned} \tag{A.2}$$

In Euclidean signature these matrices are all Hermitian.

A.2 Complete Clifford Algebra

As can be seen from A.2, not all possible combinations of Pauli matrices are present in this method. The full algebra is given by $\mathbb{1}$, the generating γ-matrices, and other independent matrices formed by taking products of the generating γ-matrices.

It is easy to convince oneself that a product symmetric under the interchange of the indices such as $\frac{1}{2}\{\gamma_\mu, \gamma_\nu\}$ can never yield a new matrix due to the anticommutator (A.1).

Therefore, new matrices can be found from antisymmetric products. The antisymmetric product is defined as

$$\gamma^{\mu_1\mu_2\cdots\mu_q} = \gamma^{[\mu_1}\cdots\gamma^{\mu_q]} := \frac{1}{q!}\sum_{\pi\in S_q}\epsilon(\pi)\gamma^{\mu_{\pi(1)}}\cdots\gamma^{\mu_{\pi(q)}} \tag{A.3}$$

where π is a permutation of the indices $\{\mu_n\}$, and the $1/q!$ guarantees the weight of such a product to be 1. The simplest such product is

$$\gamma^{\mu_1\mu_2} = \frac{1}{2}\left[\gamma^{\mu_1}, \gamma^{\mu_2}\right] = \frac{1}{2}\left(\gamma^{\mu_1}\gamma^{\mu_2} - \gamma^{\mu_2}\gamma^{\mu_1}\right) \tag{A.4}$$

These matrices together form a basis of all $2^{\lfloor N/2\rfloor}\times 2^{\lfloor N/2\rfloor}$ matrices:

$$\left\{\Gamma^A = \gamma^\mu, \gamma^{\mu_1\mu_2}, \gamma^{\mu_1\mu_2\mu_3}, \cdots, \gamma^{\mu_1\mu_2\cdots\mu_N}\right\} \tag{A.5}$$

An important property is trace orthogonality:

$$\mathrm{tr}\left(\Gamma^A\Gamma_B\right) = 2^{\lfloor N/2\rfloor}\delta^A_B \tag{A.6}$$

A.3 Product of antisymmetric products

In general, the product between $\gamma^{\mu_1\mu_2\cdots\mu_p}$ and $\gamma^{\nu_1\nu_2\cdots\nu_q}$ is found by considering the number of ways in which the indices can be contracted. One first writes down the fully antisymmetric contribution where all indices have to differ, and then conciders all possible contractions. This logic is explained in more detail in Chapter 3 of [11], here we will only state the result:

$$\begin{aligned}\gamma^{\mu_1\mu_2\cdots\mu_p}\gamma_{\nu_1\nu_2\cdots\nu_q} =& \gamma^{\mu_1\mu_2\cdots\mu_p}{}_{\nu_1\nu_2\cdots\nu_q} + C_1^{p,q}\gamma^{[\mu_1\mu_2\cdots\mu_{p-1}}{}_{[\nu_2\nu_3\cdots\nu_q}\delta^{\mu_p]}{}_{\nu_1]} \\ &+ C_2^{p,q}\gamma^{[\mu_1\mu_2\cdots\mu_{p-2}}{}_{[\nu_3\nu_4\cdots\nu_q}\delta^{\mu_{p-1}}{}_{\nu_2}\delta^{\mu_p]}{}_{\nu_1]} + \ldots\end{aligned} \tag{A.7}$$

with $C_r^{p,q} = r!\binom{p}{r}\binom{q}{r}$. Note that we are sloppy in raising and lowering the indices to make it easier to indicate which indices are mutually antisymmetric. (And since we are working with Euclidean signature, this does not matter.)

A.4 General Anti-commutator

The anticommutator between two general antisymmetric products is easily found by realizing that $\delta^{\mu\nu} = \delta^{\nu\mu}$ This means that contractions with an odd number of delta functions end up canceling each other in the anticommutator. Therefore, the result is:

$$\begin{aligned}\frac{1}{2}\left\{\gamma^{\mu_1\mu_2\cdots\mu_p}, \gamma_{\nu_1\nu_2\cdots\nu_q}\right\} =& \gamma^{\mu_1\mu_2\cdots\mu_p}{}_{\nu_1\nu_2\cdots\nu_q} + C_2^{p,q}\gamma^{[\mu_1\mu_2\cdots\mu_{p-2}}{}_{[\nu_3\nu_4\cdots\nu_q}\delta^{\mu_{p-1}}{}_{\nu_2}\delta^{\mu_p]}{}_{\nu_1]} \\ &+ C_4^{p,q}\gamma^{[\mu_1\mu_2\cdots\mu_{p-4}}{}_{[\nu_5\nu_6\cdots\nu_q}\delta^{\mu_{p-3}}{}_{\nu_4}\delta^{\mu_{p-2}}{}_{\nu_3}\delta^{\mu_{p-1}}{}_{\nu_2}\delta^{\mu_p]}{}_{\nu_1]} + \ldots\end{aligned} \tag{A.8}$$

Appendix B

Brute Force Calculation of Moments

In this chapter, the moments of some of the distributions have been calculated by brute force. The calculations use the methods of anti-symmetric products, and the fact that the χ are traceless matrices.

B.1 One Fermion Model

$$\begin{aligned}
\left\langle \mathrm{tr}\left(\mathcal{H}^2\right)\right\rangle &= \left\langle J_\mu J_\nu \mathrm{tr}\left(\chi_\mu\chi_\nu\right)\right\rangle = \left\langle J_\mu J_\nu \delta_{\mu\nu}\mathrm{tr}\left(\mathbb{1}\right)\right\rangle = \left\langle J_\mu^2\right\rangle \\
&= N\sigma^2 \\
\left\langle \mathrm{tr}\left(\mathcal{H}^4\right)\right\rangle &= \left\langle J_\mu J_\nu J_\rho J_\sigma \mathrm{tr}\left(\chi_\mu\chi_\nu\chi_\rho\chi_\sigma\right)\right\rangle = \left\langle J_\mu J_\nu J_\rho J_\sigma \mathrm{tr}\left(\left(\chi_{\mu\nu}+\delta_{\mu\nu}\right)\left(\chi_{\rho\sigma}+\delta_{\rho\sigma}\right)\right)\right\rangle \\
&= \left\langle J_\mu J_\nu J_\rho J_\sigma \mathrm{tr}\left(\cancel{2\delta^{[\rho}_{[\nu}\delta^{\sigma]}_{\mu]}} + \delta_{\mu\nu}\delta_{\rho\sigma}\right)\right\rangle = \left\langle J_\mu^2 J_\rho^2\right\rangle = \left\langle J_\mu^4\right\rangle + \binom{2}{1,1}\left\langle J_\mu^2 J_\rho^2\right\rangle \\
&= 3N\sigma^4 + N(N-1)\sigma^4 \\
&= N(N+2)\sigma^4
\end{aligned}$$

In the calculation of $\left\langle \mathrm{tr}\left(\mathcal{H}^4\right)\right\rangle$, the term $\delta^{[\rho}_{[\nu}\delta^{\sigma]}_{\mu]}$ cancels itself upon contraction with the J_μ. In the next step, $\left\langle J_\mu^2 J_\rho^2\right\rangle$, the case where $\mu=\rho$ and $\mu\neq\rho$ have to be considered separately since $\left\langle J_\mu^{2k}\right\rangle = (2k-1)!!\sigma^{2k}$ and therefore $\left\langle J_\mu^4\right\rangle \neq \left\langle J_\mu^2 J_\rho^2\right\rangle$.

Having realized this, the calculation of the next terms is greatly simplified:

$$\begin{aligned}
\left\langle \mathrm{tr}\left(\mathcal{H}^6\right)\right\rangle &= \left\langle J_\mu^2 J_\nu^2 J_\rho^2\right\rangle = \left\langle J_\mu^6\right\rangle + \binom{3}{2,1}\left\langle J_\mu^4\right\rangle\left\langle J_\rho^2\right\rangle + \binom{3}{1,1,1}\left\langle J_\mu^2\right\rangle^3 \\
&= 5!!N\sigma^6 + 3^2N(N-1) + N(N-1)(N-2)\sigma^6 \\
&= N(N+2)(N+4)\sigma^6 \\
\left\langle \mathrm{tr}\left(\mathcal{H}^8\right)\right\rangle &= \left\langle J_\mu^2 J_\nu^2 J_\rho^2 J_\sigma^2\right\rangle = \left\langle J_\mu^8\right\rangle + \binom{4}{1,3}\left\langle J_\mu^6\right\rangle\left\langle J_\nu^2\right\rangle + \binom{4}{2,2}\left\langle J_\mu^4\right\rangle\left\langle J_\nu^4\right\rangle + \\
&\qquad \binom{4}{2,1,1}\left\langle J_\mu^4\right\rangle\left\langle J_\nu^2\right\rangle\left\langle J_\rho^2\right\rangle + \left\langle J_\mu^2\right\rangle^4 \\
&= 7!!N\sigma^8 + 4\cdot 5!!N(N-1)\sigma^8 + 6\cdot 3!!^2N(N-1)\sigma^8 \\
&\quad + 3!!N(N-1)(N-2) + N(N-1)(N-2)(N-3) \\
&= N(N+2)(N+4)(N+6)\sigma^8
\end{aligned}$$

B.2 Two Fermion Model

$$\mathrm{tr}\left(\mathcal{H}^2\right) = -\frac{1}{4}J_{\mu_1\nu_1}J_{\mu_2\nu_2}\mathrm{tr}\left(\chi^{\mu_1\nu_1}\chi^{\mu_2\nu_2}\right) \tag{B.1}$$

$$= -\frac{1}{4}J_{\mu_1\nu_1}J_{\mu_2\nu_2}\mathrm{tr}\left(\chi^{\mu_1\nu_1\mu_2\nu_2} + 4\chi^{[\mu_1}{}_{[\nu_2}\delta^{\nu_1]}{}_{\mu_2]} + 2\delta^{[\mu_1}{}_{[\nu_2}\delta^{\nu_1]}{}_{\mu_2]}\right) \tag{B.2}$$

$$= -\frac{1}{4}J_{\mu_1\nu_1}J_{\mu_2\nu_2}\mathrm{tr}\left(2\delta^{[\mu_1}{}_{[\nu_2}\delta^{\nu_1]}{}_{\mu_2]}\right) \tag{B.3}$$

$$= -\frac{1}{2}\mathrm{tr}\left(\frac{1}{4}\left(2J_{\mu_1\nu_1}J_{\nu_1\mu_1} - 2J_{\mu_1\nu_1}^2\right)\right) = \frac{1}{2}J_{\mu_1\nu_1}^2\mathrm{tr}\left(\mathbb{1}\right) \tag{B.4}$$

In calculating (B.3), we have again used $C_r^{p,q}$ – the number of ways to contract r indices between two objects with p and q indices respectively.

In going from (B.3) to (B.4) we drop every term with a χ in it because only the rank 0 element (and the highest rank element in odd dimensions) has non-zero trace. Recall that since $J_{\mu\nu}$ is antisymmetric, $J_{\mu\nu}^2$ is a sum over $N(N-1)$ terms.

$$\left\langle \mathrm{tr}\left(\mathcal{H}^2\right)\right\rangle = \frac{1}{2}N(N-1)\sigma^2\mathrm{tr}\left(\mathbb{1}\right) = \binom{N}{2}\sigma^2\mathrm{tr}\left(\mathbb{1}\right) \tag{B.5}$$

$$\mathrm{tr}\left(\mathcal{H}^4\right) = \frac{1}{2^4}J_{\mu_1\nu_1}J_{\mu_2\nu_2}J_{\mu_3\nu_3}J_{\mu_4\nu_4}\mathrm{tr}\left(\chi^{\mu_1\nu_1}\chi^{\mu_2\nu_2}\chi^{\mu_3\nu_3}\chi^{\mu_4\nu_4}\right) \tag{B.6}$$

$$\begin{aligned}
&= \frac{1}{2^4}J_{\mu_1\nu_1}J_{\mu_2\nu_2}J_{\mu_3\nu_3}J_{\mu_4\nu_4}\mathrm{tr}(\\
&\qquad \left(\chi^{\mu_1\nu_1\mu_2\nu_2} + 4\chi^{[\mu_1}{}_{[\nu_2}\delta^{\nu_1]}{}_{\mu_2]} + 2\delta^{[\mu_1}{}_{[\nu_2}\delta^{\nu_1]}{}_{\mu_2]}\right) \\
&\qquad \left(\chi^{\mu_3\nu_3\mu_4\nu_4} + 4\chi^{[\mu_3}{}_{[\nu_4}\delta^{\nu_3]}{}_{\mu_4]} + 2\delta^{[\mu_3}{}_{[\nu_4}\delta^{\nu_3]}{}_{\mu_4]}\right)) \\
&= \frac{1}{2^4}J_{\mu_1\nu_1}J_{\mu_2\nu_2}J_{\mu_3\nu_3}J_{\mu_4\nu_4}\mathrm{tr}(4!\delta^{[\nu_2}_{[\mu_3}\delta^{\mu_2}_{\nu_3}\delta^{\nu_1}_{\mu_4}\delta^{\mu_1]}_{\nu_4]} \\
&\qquad + 4^2\chi^{[\mu_1}{}_{[\nu_2}\delta^{\nu_1]}{}_{\mu_2]}\chi^{[\mu_3}{}_{[\nu_4}\delta^{\nu_3]}{}_{\mu_4]} + 2^2\delta^{[\mu_1}{}_{[\nu_2}\delta^{\nu_1]}{}_{\mu_2]}\delta^{[\mu_3}{}_{[\nu_4}\delta^{\nu_3]}{}_{\mu_4]})
\end{aligned} \tag{B.7}$$

Explicit calculation shows the following rules:

$$J_{\mu_1\nu_1}J_{\mu_2\nu_2}\chi^{[\mu_1}{}_{[\nu_2}\delta^{\nu_1]}{}_{\mu_2]} = -J_{\mu_1\alpha}J_{\mu_2\alpha}\chi^{\mu_1\mu_2} \tag{B.8}$$

$$J_{\mu_1\nu_1}J_{\mu_2\nu_2}\delta^{[\mu_1}{}_{[\nu_2}\delta^{\nu_1]}{}_{\mu_2]} = -J^2_{\mu_1\nu_1} \tag{B.9}$$

The term $J_{\mu_1\nu_1}J_{\mu_2\nu_2}J_{\mu_3\nu_3}J_{\mu_4\nu_4}\delta^{[\nu_2}_{[\mu_3}\delta^{\mu_2}_{\nu_3}\delta^{\nu_1}_{\mu_4}\delta^{\mu_1]}_{\nu_4]}$ is slightly more complicated, since the antisymmetric delta function is antisymmetric under interchange of $[\nu_2\mu_2\nu_1\mu_1]$ and $[\mu_3\nu_3\mu_4\nu_4]$, but the $J_{\mu\nu}$ are only antisymmetric under subgroups of those permutations. Therefore, the possible contractions fall in one of two groups:

$$\begin{aligned} 4!J_{\mu_1\nu_1}J_{\mu_2\nu_2}J_{\mu_3\nu_3}J_{\mu_4\nu_4}\delta^{[\nu_2}_{[\mu_3}\delta^{\mu_2}_{\nu_3}\delta^{\nu_1}_{\mu_4}\delta^{\mu_1]}_{\nu_4]} &= \#J^2_{\mu_1\nu_1}J^2_{\mu_2\nu_2} + \#J_{\mu_1\nu_1}J_{\mu_2\nu_2}J_{\nu_2\nu_1}J_{\mu_1\mu_2} \\ &= 8J^2_{\mu_1\nu_1}J^2_{\mu_2\nu_2} + 16J_{\mu_1\nu_1}J_{\mu_2\nu_2}J_{\nu_2\nu_1}J_{\mu_1\mu_2} \end{aligned} \tag{B.10}$$

Plugging all this in, we obtain

$$\begin{aligned} \mathrm{tr}\left(\mathcal{H}^4\right) &= \frac{1}{2^4}\mathrm{tr}(8J^2_{\mu_1\nu_1}J^2_{\mu_2\nu_2} + 16J_{\mu_1\nu_1}J_{\mu_2\nu_2}J_{\nu_2\nu_1}J_{\mu_1\mu_2} \\ &\quad + 4^2J_{\mu_1\alpha}J_{\mu_2\alpha}\chi^{\mu_1\mu_2}J_{\mu_3\beta}J_{\mu_4\beta}\chi^{\mu_3\mu_4} + 2^2J^2_{\mu_1\nu_1}J^2_{\mu_2\nu_2}) \\ &= \frac{1}{2^4}\mathrm{tr}(12J^2_{\mu_1\nu_1}J^2_{\mu_2\nu_2} + 16J_{\mu_1\nu_1}J_{\mu_2\nu_2}J_{\nu_2\nu_1}J_{\mu_1\mu_2} \\ &\quad + 4^2J_{\mu_1\alpha}J_{\mu_2\alpha}\chi^{\mu_1\mu_2}J_{\mu_3\beta}J_{\mu_4\beta}\chi^{\mu_3\mu_4}) \end{aligned} \tag{B.11}$$

$$\left\langle \frac{12}{2^4}\mathrm{tr}\left(J^2_{\mu_1\nu_1}J^2_{\mu_2\nu_2}\right)\right\rangle = \frac{3}{4}\left[C_2^{2,2}\left\langle J^4_{\mu_1\nu_1}\right\rangle + C_1^{2,2}\left\langle J^2_{\mu_1\nu_1}\right\rangle\left\langle J^2_{\mu_1\nu_2}\right\rangle + C_0^{2,2}\left\langle J^2_{\mu_1\nu_1}\right\rangle\left\langle J^2_{\mu_2\nu_2}\right\rangle\right]\mathrm{tr}\left(\mathbb{1}\right) \tag{B.12}$$

$$\begin{aligned} &= \frac{3}{4}\sigma^4\mathrm{tr}\left(6\frac{N!}{(N-2)!} + 4\frac{N!}{(N-3)!} + \frac{N!}{(N-4)!}\right) \\ &= 3\sigma^4\left[3\binom{N}{2} + 3!\binom{N}{3} + 3!\binom{N}{4}\right]\mathrm{tr}\left(\mathbb{1}\right) \end{aligned} \tag{B.13}$$

$$\left\langle \frac{16}{2^4}\mathrm{tr}\left(J_{\mu_1\nu_1}J_{\mu_2\nu_2}J_{\nu_2\nu_1}J_{\mu_1\mu_2}\right)\right\rangle = -\left[\left\langle J^4_{\mu_1\nu_1}\right\rangle + 2\left\langle J^2_{\mu_1\nu_1}\right\rangle\left\langle J^2_{\mu_1\nu_2}\right\rangle\right]\mathrm{tr}\left(\mathbb{1}\right) \tag{B.14}$$

$$\begin{aligned} &= -\sigma^4\left[3\frac{N!}{(N-2)!} + 2\frac{N!}{(N-3)!}\right]\mathrm{tr}\left(\mathbb{1}\right) \\ &= -3\sigma^4\left[2\binom{N}{2} + 4\binom{N}{3}\right]\mathrm{tr}\left(\mathbb{1}\right) \end{aligned} \tag{B.15}$$

$$\begin{aligned} \frac{4^2}{2^4}\mathrm{tr}(J_{\mu_1\alpha}J_{\mu_2\alpha}J_{\mu_3\beta}J_{\mu_4\beta}\chi^{\mu_1\mu_2}\chi^{\mu_3\mu_4}) &= 4\mathrm{tr}(J_{\mu_1\alpha}J_{\mu_2\alpha}J_{\mu_3\beta}J_{\mu_4\beta}\delta^{[\mu_1}{}_{[\mu_4}\delta^{\mu_2]}{}_{\mu_3]}) \\ &= 2\mathrm{tr}(J_{\mu_1\alpha}J_{\mu_2\alpha}J_{\mu_2\beta}J_{\mu_1\beta} - J_{\mu_1\alpha}J_{\mu_2\alpha}J_{\mu_1\beta}J_{\mu_2\beta}) = 0 \end{aligned} \tag{B.16}$$

Therefore,

$$\left\langle \mathrm{tr}\left(\mathcal{H}^4\right)\right\rangle = 3\sigma^4\left[\binom{N}{2} + 2\binom{N}{3} + 6\binom{N}{4}\right]\mathrm{tr}\left(\mathbb{1}\right) \tag{B.17}$$

It can be checked that the anticommutator method described in the main text yields the same result. Indeed, (B.16) shows explicitly that such chaining terms do not contribute, and that is why they don't appear in the anticommutator.

B.3 Four Fermion Model

This calculation requires a little bit more planning than for the two fermion model due to the sheer number of terms created. Lets start by analyzing the product of two $\chi_{\mu\nu\rho\sigma}$:

$$\begin{aligned}\chi_{\mu_1\nu_1\rho_1\sigma_1}\chi_{\mu_2\nu_2\rho_2\sigma_2} =& \chi_{\mu_1\nu_1\rho_1\sigma_1\mu_2\nu_2\rho_2\sigma_2} + \cancel{C_1^{4,4}\chi^{[\mu_1\nu_1\rho_1}{}_{[\nu_2\rho_2\sigma_2}\delta^{\sigma_1]}_{\mu_2]}} + C_2^{4,4}\chi^{[\mu_1\nu_1}{}_{[\rho_2\sigma_2}\delta^{\rho_1}_{\nu_2}\delta^{\sigma_1]}_{\mu_2]} \\ &+ \cancel{C_3^{4,4}\chi^{[\mu_1}{}_{[\sigma_2}\delta^{\nu_1}_{\rho_2}\delta^{\rho_1}_{\nu_2}\delta^{\sigma_1]}_{\mu_2]}} + C_4^{4,4}\delta^{[\mu_1}_{[\sigma_2}\delta^{\nu_1}_{\rho_2}\delta^{\rho_1}_{\nu_2}\delta^{\sigma_1]}_{\mu_2]} \qquad \text{(B.18)}\end{aligned}$$

Since the anticommutator method shows that the terms containing an odd number of contractions end up canceling, they have been displayed as canceled in (B.18). And since the χ are traceless, the calculation of $\langle \mathrm{tr}\left(\mathcal{H}^2\right)\rangle$ simply becomes

$$\begin{aligned}\langle \mathrm{tr}\left(\mathcal{H}^2\right)\rangle &= \frac{4!}{(4!)^2}\left\langle J^2_{\mu_1\nu_1\rho_1\sigma_1}\mathrm{tr}\left(\mathbb{1}\right)\right\rangle \\ &= \frac{1}{4!}N(N-1)(N-2)(N-3)\sigma^2\mathrm{tr}\left(\mathbb{1}\right) = \binom{N}{4}\sigma^2\mathrm{tr}\left(\mathbb{1}\right)\end{aligned}$$

For $\langle \mathrm{tr}\left(\mathcal{H}^4\right)\rangle$, (B.18) has to be squared. In anticipation of taking the trace, only products containing χ of equal rank will be written down, since it it is easy to show that a product of χ's of unequal rank will be traceless.

$$\begin{aligned}&(\chi_{\mu_1\nu_1\rho_1\sigma_1}\chi_{\mu_2\nu_2\rho_2\sigma_2})(\chi_{\mu_3\nu_3\rho_3\sigma_3}\chi_{\mu_4\nu_4\rho_4\sigma_4}) \to \\ &\qquad \chi_{\mu_1\nu_1\rho_1\sigma_1\mu_2\nu_2\rho_2\sigma_2}\chi_{\mu_3\nu_3\rho_3\sigma_3\mu_4\nu_4\rho_4\sigma_4} \\ &\qquad + (C_2^{4,4})^2\chi^{[\mu_1\nu_1}{}_{[\rho_2\sigma_2}\delta^{\rho_1}_{\nu_2}\delta^{\sigma_1]}_{\mu_2]}\chi^{[\mu_3\nu_3}{}_{[\rho_4\sigma_4}\delta^{\rho_3}_{\nu_4}\delta^{\sigma_3]}_{\mu_4]} \\ &\qquad + (C_4^{4,4})^2\delta^{[\mu_1}_{[\sigma_2}\delta^{\nu_1}_{\rho_2}\delta^{\rho_1}_{\nu_2}\delta^{\sigma_1]}_{\mu_2]}\delta^{[\mu_3}_{[\sigma_4}\delta^{\nu_3}_{\rho_4}\delta^{\rho_3}_{\nu_4}\delta^{\sigma_3]}_{\mu_4]}\end{aligned}$$

$$\begin{aligned}&(\chi_{\mu_1\nu_1\rho_1\sigma_1}\chi_{\mu_2\nu_2\rho_2\sigma_2})(\chi_{\mu_3\nu_3\rho_3\sigma_3}\chi_{\mu_4\nu_4\rho_4\sigma_4}) \to \\ &\qquad C_8^{8,8}\delta^{[\mu_1}_{[\sigma_4}\delta^{\nu_1}_{\rho_4}\delta^{\rho_1}_{\nu_4}\delta^{\sigma_1}_{\mu_4}\delta^{\mu_2}_{\sigma_3}\delta^{\nu_2}_{\rho_3}\delta^{\rho_2}_{\nu_3}\delta^{\sigma_2]}_{\mu_3]} \qquad \text{(B.19)} \\ &\qquad + (C_2^{4,4})^2\chi^{[\mu_1\nu_1}{}_{[\rho_2\sigma_2}\delta^{\rho_1}_{\nu_2}\delta^{\sigma_1]}_{\mu_2]}\chi^{[\mu_3\nu_3}{}_{[\rho_4\sigma_4}\delta^{\rho_3}_{\nu_4}\delta^{\sigma_3]}_{\mu_4]} \qquad \text{(B.20)} \\ &\qquad + (C_4^{4,4})^2\delta^{[\mu_1}_{[\sigma_2}\delta^{\nu_1}_{\rho_2}\delta^{\rho_1}_{\nu_2}\delta^{\sigma_1]}_{\mu_2]}\delta^{[\mu_3}_{[\sigma_4}\delta^{\nu_3}_{\rho_4}\delta^{\rho_3}_{\nu_4}\delta^{\sigma_3]}_{\mu_4]} \qquad \text{(B.21)}\end{aligned}$$

Firstly, (B.20) and (B.21) look very similar to their two fermion counterpart. (B.21) will fully contract with the $J_{\mu\nu\rho\sigma}$ to form $(4!)^2\left\langle J^2_{\mu_1\nu_1\rho_1\sigma_1}J^2_{\mu_2\nu_2\rho_2\sigma_2}\right\rangle$. (B.20) will be zero upon contraction with the $J_{\mu\nu\rho\sigma}$ for the same reason that (B.16) is zero.

This leaves (B.19) to be analyzed. Similar to (B.10), the terms will fall into

one of four categories:

$$
\begin{aligned}
J_{\mu_1\nu_1\rho_1\sigma_1}J_{\mu_2\nu_2\rho_2\sigma_2}J_{\mu_3\nu_3\rho_3\sigma_3}J_{\mu_4\nu_4\rho_4\sigma_4}C_8^{8,8}\delta^{[\mu_1}_{[\sigma_4}\delta^{\nu_1}_{\rho_4}\delta^{\rho_1}_{\nu_4}\delta^{\sigma_1}_{\mu_4}\delta^{\mu_2}_{\sigma_3}\delta^{\nu_2}_{\rho_3}\delta^{\rho_2}_{\nu_3}\delta^{\sigma_2]}_{\mu_3]} = \\
&+ 2(4!)^2 J^2_{\mu_1\nu_1\rho_1\sigma_1}J^2_{\mu_2\nu_2\rho_2\sigma_2} \\
&- \#J_{\mu_1\nu_1\rho_1\sigma_1}J_{\mu_2\nu_2\rho_2\sigma_2}J_{\mu_1\nu_1\rho_1\mu_2}J_{\sigma_1\nu_2\rho_2\sigma_2} \\
&+ \#J_{\mu_1\nu_1\rho_1\sigma_1}J_{\mu_2\nu_2\rho_2\sigma_2}J_{\mu_1\nu_1\mu_2\nu_2}J_{\rho_1\sigma_1\rho_2\sigma_2} \\
&- \#J_{\mu_1\nu_1\rho_1\sigma_1}J_{\mu_2\nu_2\rho_2\sigma_2}J_{\mu_1\mu_2\nu_2\rho_2}J_{\nu_1\rho_1\sigma_1\sigma_2}
\end{aligned}
$$

The $2(4!)^2$ is obtained by considering that there are two groups of indices in the delta product that are antisymmetric under interchange in the J, making the total symmetric, and that these groups appear twice. In principle it should be possible to determine the exact number of terms in each of the other groups as well. However, since they are all subleading, we shall just assume large N now, and drop all but the first (leading) term. Putting everything together, we get:

$$
\begin{aligned}
\left\langle \mathrm{tr}\left(\mathcal{H}^4\right)\right\rangle &\approx \frac{3(4!)^2}{(4!)^4}\left\langle J^2_{\mu_1\nu_1\rho_1\sigma_1}J^2_{\mu_2\nu_2\rho_2\sigma_2}\right\rangle \mathrm{tr}\left(\mathbb{1}\right) \\
&\approx \frac{3(4!)^2}{(4!)^4}\left\langle J^2_{\mu_1\nu_1\rho_1\sigma_1}\right\rangle\left\langle J^2_{\mu_2\nu_2\rho_2\sigma_2}\right\rangle \mathrm{tr}\left(\mathbb{1}\right) = 3\sigma^4\binom{N}{4}\binom{N-4}{4}\mathrm{tr}\left(\mathbb{1}\right) \\
&\approx 3\sigma^4\binom{N}{4}^2\mathrm{tr}\left(\mathbb{1}\right)
\end{aligned}
$$

In this last step some overcounting has been done but the large N behavior is identical and this is notationally more consistent.

Bibliography

[1] A. Almheiri, D. Marolf, J. Polchinski, and J. Sully, "Black holes: Complementarity or firewalls?," *Journal of High Energy Physics* **2013** no. 2, (2013) 1–19, arXiv:1207.3123.

[2] D. Harlow, "Jerusalem lectures on black holes and quantum information," *Reviews of Modern Physics* **88** no. 1, (2016) , arXiv:1409.1231.

[3] J. Maldacena, "The Large N Limit of Field Theories and Gravity," arXiv:9711200 [hep-th].

[4] J. Maldacena, S. H. Shenker, and D. Stanford, "A bound on chaos," *Journal of High Energy Physics* **2016** no. 8, (2016) , arXiv:1503.01409v1.

[5] P. Hayden and J. Preskill, "Black holes as mirrors: quantum information in random subsystems," *Journal of High Energy Physics* **2007** no. 09, (2007) 120–120, arXiv:0708.4025.

[6] Y. Sekino and L. Susskind, "Fast scramblers," *Journal of High Energy Physics* **2008** no. 10, (2008) 065–065, arXiv:0808.2096.

[7] L. Susskind, "Addendum to Fast Scramblers," *Physics* (2011) 16, arXiv:1101.6048.

[8] N. Lashkari, D. Stanford, M. Hastings, T. Osborne, and P. Hayden, "Towards the fast scrambling conjecture," *Journal of High Energy Physics* **2013** no. 4, (2013) , arXiv:1111.6580.

[9] A. Kitaev, "A simple model of quantum holography," in *KITP strings seminar and Entanglement 2015 program*. 2015. http://online.kitp.ucsb.edu/online/entangled15/.

[10] J. Maldacena and D. Stanford, "Comments on the Sachdev-Ye-Kitaev model," arXiv:1604.07818.

[11] D. Z. Freedman and A. V. Proeyen, *Supergravity*. 2012.

[12] J. Polchinski, *String Theory*, vol. B. 1998.

[13] J. Polchinski and V. Rosenhaus, "The spectrum in the Sachdev-Ye-Kitaev model," *Journal of High Energy Physics* **2016** no. 4, (2016) 1, arXiv:1601.06768.

[14] S. H. Shenker and D. Stanford, "Black holes and the butterfly effect," *Journal of High Energy Physics* **2014** no. 3, (2014) 0–30, arXiv:1306.0622.

[15] B. De Wit and J. Smith, *Field Theory in Particle Physics - Appendix E*.

[16] A. B. de Monvel and A. Khorunzhy, "Some elementary results around the Wigner semicircle law,". https://www.physik.uni-bielefeld.de/bibos/old-bibos-site/01-03-035.pdf.

[17] F. Oravecz, "Symmetric Partitions and Pairings," *Colloquium Mathematicum* **104** no. 1, (2006) 113–140.